The functional database of the ARCHI project: Potential and perspectives

Philippe Pinel [a,*], Baudouin Forgeot d'Arc [b,c], Stanislas Dehaene [a,d,e], Thomas Bourgeron [f,g,h], Bertrand Thirion [i,j,d], Denis Le Bihan [j], Cyril Poupon [j]

[a] INSERM U992, NeuroSpin, CEA, 91191, Gif-sur-Yvette, France
[b] CHU Ste-Justine Research Center, Montréal, Quebec, H3T 1C5, Canada
[c] Department of Psychiatry, Université de Montréal, Montréal, Quebec, H3C 3J7, Canada
[d] Université Paris-Saclay, 91191, Gif-sur-Yvette, France
[e] Collège de France, 75005, Paris, France
[f] Human Genetics and Cognitive Functions Unit, Institut Pasteur, 75015, Paris, France
[g] CNRS UMR3571, Genes, Synapses and Cognition, Institut Pasteur, 75015, Paris, France
[h] Human Genetics and Cognitive Functions, Université Paris Diderot, Sorbonne Paris Cite, 75013, Paris, France
[i] Parietal Team, Inria, 91191, Gif-sur-Yvette, France
[j] NeuroSpin, CEA, 91191, Gif-sur-Yvette, France

A R T I C L E   I N F O

A B S T R A C T

More than two decades of functional magnetic resonance imaging (fMRI) of the human brain have succeeded to identify, with a growing level of precision, the neural basis of multiple cognitive skills within various domains (perception, sensorimotor processes, language, emotion and social cognition …). Progress has been made in the comprehension of the functional organization of localized brain areas. However, the long time required for fMRI acquisition limits the number of experimental conditions performed in a single individual. As a consequence, distinct brain localizations have mostly been studied in separate groups of participants, and their functional relationships at the individual level remain poorly understood. To address this issue, we report here preliminary results on a database of fMRI data acquired on 78 individuals who each performed a total of 29 experimental conditions, grouped in 4 cross-domains functional localizers. This protocol has been designed to efficiently isolate, in a single session, the brain activity associated with language, numerical representation, social perception and reasoning, premotor and visuomotor representations. Analyses are reported at the group and at the individual level, to establish the ability of our protocol to selectively capture distinct regions of interest in a very short time. Test-retest reliability was assessed in a subset of participants. The activity evoked by the different contrasts of the protocol is located in distinct brain networks that, individually, largely replicate previous findings and, taken together, cover a large proportion of the cortical surface. We provide detailed analyses of a subset of regions of relevance: the left frontal, left temporal and middle frontal cortices. These preliminary analyses highlight how combining such a large set of functional contrasts may contribute to establish a finer-grained brain atlas of cognitive functions, especially in regions of high functional overlap. Detailed structural images (structural connectivity, micro-structures, axonal diameter) acquired in the same individuals in the context of the ARCHI database provide a promising situation to explore functional/structural interdependence. Additionally, this protocol might also be used as a way to establish individual neurofunctional signatures in large cohorts.

1. Introduction

Understanding the functional organization of the human cerebral cortex remains a major scientific challenge. The switch of interest from single-case brain lesion studies to neuroimaging group studies has enhanced generalization and reproducibility of findings. However, it might have led to a new series of challenges. First, exploring cognitive functions using different tasks in independent studies (i.e. in different groups, scanners, etc.) limits comparisons between functional circuits, consequently preventing any firm conclusion from being drawn on the topographical relations between functional correlates (Amunts et al., 2014). The problem is obvious, for instance, in the superior temporal lobes (STS) (Hein and Knight, 2008), the medial frontal and the prefrontal cortex (de la Vega et al., 2016) which are repeatedly activated in a huge range of experimental conditions such as attention orientation, social tasks, and language processing. This spatial concentration and overlap between seemingly distinct functions raise the question of shared neural mechanisms between different cognitive domains (van den Heuvel and Sporns, 2013). Identifying these nodes is crucial to better understand their respective functions. Hence, exploring the local geometrical organization of activation maps across cognitive domains may enlighten the development and interdependence of our cognitive abilities. Second, group analyses over several subjects erase interindividual variability and reduce activity maps to an average representation, underestimating individual complexity of functional patterns (lateralization, size, shape, and a number of activated clusters) (Nadeau et al., 1998; Thirion et al., 2007). However, repeated individual acquisitions in similar experimental situations have shown that the complex individual functional mosaics could be reproduced over sessions, although they remain poorly understood (Miller et al., 2009). Nowadays the understanding of the fine organization of multiple cortical areas at the single subject level remains a limitation of the fMRI approach (Laumann et al., 2015). Third, individual functional variability parallels anatomical differences (cortical fiber projection, sulcus shape) (Hill et al., 2010; Putnam et al., 2010; Saygin et al., 2012; Sun et al., 2016). This tight interdependence might locally clarify some functional organization (Behrens et al., 2006) making it essential to study brain structure and activity in the same individuals. Characterizing individual differences then requires a large functional multi-domain design, as well as a range of structural images, fine anatomy, sulci description, and diffusion tensor imaging (DTI). Thus, there is an increasing need for databases containing sets of individual functional maps along with anatomical structure.

We previously developed a first large-scale database of hundreds of participants based on a localizer designed to identify correlates of reading, speech listening, mental calculation, primary visual perception, and motor action. Participants only performed ten trials per condition, but this multifunctional database successfully allowed to identify a subtle relationship between math and language networks lateralization, and the impact of genetic variations on language correlates (Pinel et al., 2007, 2012). Recently, other initiatives contributed to the same effort and increased the variety of cognitive fields explored: the IMAGEN project (Schumann et al., 2010) aimed to scan 2000 adolescents to understand their brain development and behavior, using condition encompassed in the Pinel et al. localizer (2007) plus two decision tasks and face observation. The Human Connectome Project (HCP) database (Van Essen et al., 2012) includes functional maps covering up to seven different cognitive domains together with resting state, T1- and T2-weighted MRI (fiber bundles, anatomical parameters such as maps of myelin or cortical thickness) and magnetoencephalography/electroencephalography (MEG/EEG) in a large cohort of subjects. The present article describes the rationale of a new fMRI database, composed of scans from 78 healthy subjects, which complements measures of connectivity acquired from the same individuals at the NeuroSpin center in the context of the CONNECT project (Consortium Of Neuroimagers for the Non-invasive Exploration of brain Connectivity and Tracts) (Assaf et al., 2013), a consortium aimed at integrating knowledge on brain tractography and tissue microstructure. The CONNECT project produced various atlases of connectivity, such as brain white matter tracts, axonal density and diameter, and myelin. This was an ideal situation to understand how structural constraints carve functional territories or evolve jointly, and how complex individual functional networks relate to anatomical variability. Indeed, the fine structure of short-range connections might play a role in the organization of functional nodes and modules (van den Heuvel and Sporns, 2013). We then extended our previous localizer to two additional functional domains (social tasks and visuomotor tasks), developing a set of four localizer protocols that contribute to cover a large number of cortical regions in the shortest possible time.

The new localizers were aimed at identifying the cerebral bases of a large range of human cognitive skills, using robust paradigms. They were designed to evoke visuospatial processes (from ocular saccade up to mental shape manipulation), fine motor preparation (grasping) and social cognition (emotion recognition, theory of mind (ToM), intention perception). Taken together, these tasks should help to activate most of the cortical surface and subcortical structures. A particular effort was made in our choice to produce, at the individual level, a rough functional mosaic of the superior parietal and the temporal lobe. Indeed, sulci structures of these brain areas present complex and quite variable shapes (size, segmentation) (Ochiai et al., 2004; Zlatkina and Petrides, 2014). Adding a detailed functional mapping of these regions may help to understand these complex patterns.

Here, we introduce the potential of this multi-domain database by presenting a description of the available protocols as well as a preliminary analysis performed on 78 subjects at group and individual levels. We present detailed functional atlases covering regions of particular interest such as the superior parietal cortex, temporal gyrus, lateral prefrontal medial cortex and the medial surface of cerebral hemisphere. This material will allow to generate new multidimensional analysis in the future and will provide an opportunity to make comparison/prediction with data from the other databasing projects mentioned above.

2. Materials & methods

2.1. Subjects and scanning procedure

2.1.1. The ARCHI cohort

Functional MRIs are part of the ARCHI database project acquired from and stored in NeuroSpin center in the context of the CONNECT project. Seventy-nine healthy individuals (mean age: 23.5 years [18–40]; 47 men, 32 women; 76 right-handed and 3 left-handed) participated in the protocol. One did not perform the fMRI sessions, resulting in 78 subjects with localizers acquisitions. Each subject attended three sessions: two sessions were dedicated to anatomical acquisitions (fine anatomical volumes, DTI), which will not be discussed in the present report (see details in (Assaf et al., 2013)), and one to functional activations mapping. Images from the anatomical acquisition were processed to generate an atlas of brain connectivity and microstructures (axonal density, axonal diffusivity, myelin water fraction) provided in standardized space. The functional acquisition consisted of four functional localizers, performed in an apparently random order, and a T1-weighted structural MRI. This session lasted about 80–90 min.

Participants were first briefed and trained outside the scanner on a few sample trials (5 min), to enhance task comprehension, rapid responses and ability to restrict movement amplitude (when a motor response was required, such as in the grasping task). After scanning, participants were questioned and tested on their perception and understanding, especially on tasks that did not require any responses during fMRI acquisition, as in the false belief task (2–3 min). The training and debriefing material is available on https://philippepinel.wixsite.com/localizers. Before starting each localizer acquisition, subjects were reminded of the tasks to be done with instructions and examples displayed within the scanner (1–2 min). This procedure ensured that

subjects were not confused, considering the high number of experimental conditions.

Individual genetic material was collected for subsequent analysis, from a saliva sample, using the DNA collection kit (OG-250, DNA Genotek®). DNA was extracted according to the manufacturer's instructions. Genetic material processing and analysis will not be discussed in the article.

2.1.2. The Individual Brain Charting dataset

To assess the reliability of our protocol, we used the functional data from the Individual Brain Charting (IBC) dataset which identically replicates the present protocol in an independent, smaller set of 13 individuals (Pinho et al., 2018) (Two females, age ranging between 26 and 40 years– median = 34.5 years). Subjects performed two to four sessions of each task, which provides a rich test/re-test situation.

2.2. Tasks choice

As stated before, we aimed to cover a large proportion of cortical and subcortical structures, with a refined mapping of the parietal and posterior temporal regions, where a high degree of convergence and overlapping circuits have been previously reported (Culham and Kanwisher, 2001; Decety and Lamm, 2007; Hein and Knight, 2008; Liebenthal et al., 2014). Here, we briefly detail the main targeted brain structures. *Language correlates*: As in our original localizer protocol (Pinel et al., 2007), participants were presented audio and video (written) sentences to ensure identification of the core language system, including Wernicke's and Broca's area, precentral gyrus, extended activations along the superior temporal sulci, and subcortical nuclei (Thalamus, hippocampus). The conjunction of an audio and a visual task was aimed to identify the part of the network that was independent of the modalities used. Additionally, the visual task was predicted to evoke a ventral temporal activation usually referred to as the visual word form area (VWFA) (Cohen and Dehaene, 2004), whereas speech listening was predicted to activate the primary auditory cortex. *Frontoparietal circuits*: We selected some of the tasks previously used to map the superior parietal lobe (Simon et al., 2002): objects grasping, ocular saccades and mental arithmetic were reported to activate the superior parietal lobe (SPL) and intraparietal sulcus (IPS), revealing an antero-posterior functional gradient. Interestingly, these tasks also activate mirror regions in the frontal cortex (Simon et al., 2004). We also included a task of mental manipulation of hand images, previously used to assess mechanisms supporting motor imagery (Cohen et al., 1996; Jordan et al., 2001) and premotor representation (Kosslyn et al., 1998; Rusconi et al., 2009). *Social cognition*: This is an umbrella term for a vast collection of functions crucial for social interactions, ranging from automatic processing of perceptual cues (vocalizations, faces or movements) up to active psychological inferences on the others' states of mind. We built four tasks based on classical paradigms that had been previously shown to elicit different aspects of social cognition: detection of speaker's identity and emotional state evoked by hearing human vocalizations (Belin et al., 2000), attribution of intention to animated shapes (Castelli et al., 2000; Heider and Simmel, 1944), judgment of faces to extract internal states (Baron-Cohen et al., 1999) or traits (Winston et al., 2002) and short stories involving false beliefs (Baron-Cohen et al., 1985; Fletcher et al., 1995; Saxe and Kanwisher, 2003). Those tasks have been previously associated with different brain circuits, noticeably such as the posterior superior temporal sulcus (pSTS) region, temporoparietal junction (TPJ), medial prefrontal cortex (mPFC), orbitofrontal cortex (OFC), precuneus/posterior cingulate cortex (pCC) and amygdala (Baron-Cohen et al., 1999; Perner and Aichhorn, 2008; Saxe, 2006). Finally, we also used two additional tasks already included in our original localizer: motor action with left and right hands, ensuring activation of the sensorimotor cortices, cerebellum and thalamus, and basic visual stimulation using vertical and horizontal checkerboards: contrasting visual and horizontal checkerboards isolates V1 areas, as well as V1/V2, V3/V3A and V1.V2d borders (Pinel et al., 2007).

2.3. Tasks procedures

The above tasks were distributed in four localizers, programmed using E-Prime 1 and 2 (Psychology Software tools, Pittsburgh, PA, USA). The contrasts (difference between task of interest and control task) were chosen so that they are loose enough to robustly reproduce activations previously identified in the literature, while being able to identify specific neural components. In total, 29 tasks were performed (see E-Prime scripts and stimuli on https://philippepinel.wixsite.com/localizers). A fixed order for the presentation of trials was computed with a genetic algorithm already used in our 2007 localizer (Pinel et al., 2007), and 20% of blank trials (null event) and variable jittering were introduced, following recommendations for the optimization of fMRI design (Wager and Nichols, 2003).

Pinel et al., 2007 Localizer. This five-minute localizer has been shown to reliably isolate brain correlates of (a) covert video sentence reading, (b) audio sentence listening, (c) hand motor action, (d) mental calculation and (e) flashed checkerboards (see details in Pinel et al., 2007). Tasks were presented in a fast event-related design, alternating with a fixed random order. The video sentence task consisted of reading silently 10 sentences presented in 4 groups of one to three words, successively displayed for 250 ms each, separated by a 100 ms interval, resulting in 1.3 s of visual stimulation. During the audio sentence listening task, 10 audio sentences, comparable in length to the video sentences, were passively listened by the subjects. In motor action tasks, participants were asked to press five times on a button with left or right hand using their thumb, following video or audio instruction (for instance "press three times on the left button" where they had to press button with the left thumb). Experimental situations were equally split: 10 were presented with audio instruction (5 audio right hand and 5 audio left hand actions) and 10 were presented with video instructions (5 video right hand and 5 video left hand actions). Mental calculation trials were presented either in video (10 video calculation trials) or audio mode (10 audio calculation trials). Participants were asked to solve the arithmetical problem and silently enounce the result. Primary visual stimulation was composed of a passive succession of 5 vertical (V) checkerboards and 5 horizontal (H) flashing checkerboards, consisting of a series of 8 alternated black and white images flashed for 200 ms. After each trial, an additional jitter was added for a better sampling of hemodynamic signal and an accurate reconstruction of blood oxygen level dependent responses after signal deconvolution ([0.5–2.2 s]).

The social cognition localizer. It was composed of tasks aimed to elicit ToM, animacy and human voice recognition, plus their respective control conditions. They were presented in a fixed random order, following a fast event-related design: (a) the story comprehension task, targeting ToM, was adapted from the false belief paradigm (Wimmer and Perner, 1983) and presented in auditory (Audio false belief task – 5 trials) and visual modality (Video false belief task – 5 trials), with control sentences implying physical explanation presented in auditory (Audio mechanical task – 5 trials) and visual modality (Video mechanical task – 5 trials); (b) the animacy task, inspired by classical paradigms (Castelli et al., 2002; Heider and Simmel, 1944) and composed of movies representing animated triangles displaying intentional interaction (intentional triangles task – 10 trials) or with random movement (random triangles task – 10 trials); (c) the sound task, based on stimuli selected from the Belin et al. experiment (Belin et al., 2000) including human vocalizations (vocalization task – 10 trials), non human sounds (non-human sounds task – 10 trials) and blank trials (15 trials). In the visual modality, false belief and mechanical tasks were presented in a serie of 6 successive screens, each displaying a group of 2–5 words, in white letters on a black background. Screens were displayed during 700 ms separated by a 120 ms interval. The series was followed by an 830 ms pause and a screen displaying the word "Why?" during 1300 ms (see Supplementary Fig. 1). The stories described an initial situation and an outcome. The question "why" asked about the explanation of the outcome, that could be either a false belief from one of the characters (i.e "Stefan has versed ketchup on

his arm. Her mother saw him and ran towards him with an emergency kit. Why?"') or a physical event (i.e "Pierre is skating on the frozen lake. Later, Pierre returns home soaking wet. Why?"). Subjects were instructed to silently enounce a plausible reason to explain the situation in a few words (i.e "the mother thought it was blood" for the false belief example, and "because the ice broke and Pierre fell into the water" for the mechanical story). Auditory sentences followed the same structure for both the false belief and the mechanical tasks. Each trial duration was 8500 ms. The animacy task was composed of short animations (6500 ms) of two white triangles moving on a black screen (see Supplementary Fig. 1). The animations were created using flash Pro 2008® so that, in the intentional condition, the triangles are typically interpreted as agents interacting (e.g. pursuing, fighting, petting each other) while in the control condition, the triangles seem to move randomly. In the sound tasks, auditory stimuli were presented for 6000 ms. Vocalizations consisted of various non-speech sounds produced by humans (e.g. sneeze, laugh, cough) while the non-human sounds came from animals or a mechanical origin (e.g. dog, train, bell). Blank trials consisted of a white cross displayed in the screen center for 3000 ms. After each trial, an additional jitter was added ([0–0.8 s]).

The Social Face Localizer. It was composed of tasks based on face processing, organized as a fast event-related design mixed in a fixed random order (see Supplementary Fig. 2): (a) A version of the eyes task was adapted from the read the mind in the eyes test (Baron-Cohen et al., 1997). Participants were asked to determine intention (Eyes intention task – 10 trials) or gender (Eyes gender task – 10 trials) from a black and white picture of an individual's eyes region, or to determine the orientation of a scrambled image (Scrambled eyes tasks – 5 trials). All trials of this localizer followed the same sequence: a written question was displayed in the center of the screen for 1200 ms, successively followed by a black screen (150 ms), the image (600 ms) and a black screen again (1100 ms). This sequence was repeated twice (with two different images). Prior to the experiment, participants were asked to select and silently enounce the correct answer. In the eyes task, participants were asked to choose between two mental states (i.e "angry or preoccupied?"). In the gender eyes task, the stimuli were similar, but the participants were asked to choose between "man or woman?". In the eyes control task, similar pictures had been scrambled, half of them inclined on a 4-degree angle and the question was "straight or inclined?". In the trustworthiness task, the question was "would you feel comfortable with this person?". Images were black and white photographs of neutral faces (from man or woman) from the Karolinska face databank (Lundqvist et al., 1998). We selected ten faces with the 5 lowest and 5 highest ratings for trustworthiness, based on a previous study (Oosterhof and Todorov, 2008). The face gender task used same stimuli preceded by the question "man or woman?". In the face control task, face photographs were scrambled, half of them inclined on a 4° angle and the question was "straight or inclined?". Blank trials consisted in a white cross displayed in the center of the screen for 4850 ms. Each trial was followed by an additional jitter [0–2 s].

The Parietal Localizer. It was composed of five tasks of interest and control: (a) 8 blocks (3 trials each) of an object grasping task and 8 blocks (3 trials each) of its control task (inclination task), (b) 8 blocks (3 trials each) of the hand rotation task and 8 blocks (3 trials each) of its control task (hand side task) and (c) 8 blocks (4 trials each) of the saccades task (see Supplementary Fig. 3). Theses blocks appeared in a fixed random order and were separated by a variable period (jitter average = 4 s, [0–8 s]). For the grasping task, blocks started with an instruction (700 ms) asking to mimic a right-hand grasping gesture adapted for each presented object, without moving their wrist. Stimuli were black and white pictures of common objects such as a clamp, teapot, vaporizer, needle, etc. requiring various grasping sizes and hand configurations. Images were displayed in the center of the screen in a white frame (equally leftward or rightward oriented) on a black background. The structure of the control task (inclination task) was similar except for the initial instruction, which was to mimic with the right hand the

orientation of the frame. Stimuli were similar to the grasping stimuli but sorted from another set. All trials were separated by 1200 ms. For the hand rotation task, a block started with an instruction (700 ms) asking to silently figure out if the stimulus depicted a left or a right hand. Stimuli randomly selected among 14 pictures of left hand and 14 of right hand, rotated by either 90°, 120°, 150°, 180°, 210°, 240° or 270°. The structure of the control task (hand side task) was similar except for the initial instruction, asking to silently decide if the stimulus was the back or the palm of a hand. Stimuli were similar to the hand rotation task but sorted from another set. All trials were separated by 1200 ms. For the saccades block, the central fixation cross moves for 400 ms to a peripheral site, while a grey marker still indicated the screen center, and then it comes back to the center for 1175 ms. Subjects were instructed to follow the cross, with their eyes. Eight peripheral locations were possible, equally distributed at equal distance from the center.

2.4. Data acquisition and preprocessing

We used a 3-Tesla MRI (Siemens Trio TIM) with a 12-channel head coil, and a gradient-echo planar imaging sequence sensitive to brain oxygen level dependent contrast (40 contiguous axial slices, acquired using ascending interleaved sequence, 3 mm thickness; TR (repetition time) = 2400 ms; flip angle = 90°, TE (echo time) = 30 ms, in-plane resolution = 3×3 mm, matrix = 64×64). For each acquisition, the first four volumes were discarded to reach equilibrium. T1-weighted images were also acquired for anatomical localization. Data were preprocessed using SPM5 software (http://www.fil.ion.ucl.ac.uk/spm/) as follows: Images were converted from DICOM to nifty format. The SPM FieldMap toolbox was applied for correcting distortions caused by static field inhomogeneities (TE1 = 10 ms/TE2 = 12.46 ms/EPI readout time = 30.72 ms). The SPM slice timing correction was applied to each 3D volume to compensate acquisition delays between slices (sequential ascending order, first slice as reference). Individual movements were estimated and corrected using a rigid realignment (least squares approach) of all functional images onto the first one of the time-series (average translation movements and standard deviation in mm: along x axis = 0.4 (max = 1.5, std = 0.2), y axis = 0.6 (max = 2.2, std = 0.4), z axis = 1.3 (max = 6.3, std = 1.0); average rotation movements and standard deviation in degree: pitch = 1.3 (max = 9.7, std = 1.3), roll = 0.6 (max = 1.4, std = 0.3), yaw = 0.5 (max = 1.6, std = 0.3)). To evaluate global instantaneous head motion as a scalar quantity, we used the Framewise Displacement (FD) introduced by Power et al. (2012) and computed as follows: $FD_i = |\Delta(x_i)| + |\Delta(y_i)| + |\Delta(pitch_i)| + |\Delta(roll_i)| + |\Delta(yaw_i)|$ where, for instance, $|\Delta(x_i)| = x(\text{acquisition } i) - x(\text{acquisition } i\text{-}1)$ (rotation movement being converted from degree to millimeters). For each subject, we calculated the average of |FD vector|. Across subjects, mean individual FD = 0.05 mm (std = 0.02).

T1 anatomical image was normalized onto the MNI template (ICBM152 - Montreal Neurological Institute) using linear (12-parameter affine) and non-linear transformations (warping). We applied the resulting transformation matrix onto EPI images once coregistered to the native T1-weighted image. Normalized functional images were resampled (voxel size = $3 \times 3 \times 3$ mm) and finally smoothed (5 mm FWHM) to increase the signal-to-noise (see the detailed method in https://www.fil.ion.ucl.ac.uk/spm/doc/books/hbf2). One subject was excluded from the Social Face Localizer analysis because he dropped out of the experiment during the course of that block.

The data of the IBC dataset were acquired with a different MRI scanner (Siemens Prisma vs Trio), a different sequence (Multiband factor of 3, in-place acceleration of 2) and have a higher resolution (1.5 mm isotropic). The preprocessing pipeline is mostly identical to that of the ARCHI dataset (Pinho et al., 2018). The maps used are publicly available on NeuroVault (https://neurovault.org/) under the collection #4438. They were masked by a grey matter image. Note that the localizer protocols were designed under another name in the Pinho et al. paper: "ARCHI Standard task" corresponds here to the Pinel et al., 2007

Localizer, "ARCHI Spatial" corresponds to the Parietal Localizer, "ARCHI Social" corresponds to the Social Cognition Localizer and "ARCHI Emotional" corresponds to the Social Face Localizer.

These protocols were run at least twice: one time for an Anterior to Posterior (AP) and one time for a Posterior to Anterior (PA) phase encoding. This protocol was designed to ensure within-subject contrast replication while mitigating potential limitations concerning the distortion-correction procedure. The Pinel et al., 2007 and Parietal Localizers were systematically repeated four times (2 AP and 2 PA sessions), the Social Cognition was repeated four times in only 5 subjects and Social Face Localizers only two times.

2.5. Individual functional images

Brain responses evoked by the different experimental conditions (task) were modeled using SPM analysis tools. An individual design matrix was created with the 729 images, four sessions, and 29 tasks. Within a session, each voxel time series was fitted with a linear combination of functions, derived by convolving a standard SPM hemodynamic response function (hrf) with the time series of the tasks onsets, plus its temporal derivative. Individual functional contrast images were then computed by comparing estimated coefficients of each task ($_T$) vs. rest and between each task of interest and its control (comparing, for instance, a face task with a scrambled face task, as described below). Contrasts' names used in the results section correspond to the computation of the following vectors in the SPM design matrix: calculation = (audio calculation $_T$ + video calculation $_T$ - audio sentence $_T$ - video sentence $_T$), video sentence = video sentence $_T$ - (V & H checkerboard $_T$), audio sentences = (audio sentences $_T$ - rest), audio Right (R) hand = (audio right hand $_T$ – rest), video right (R) hand = (video right hand $_T$ - rest), audio left (L) hand = (audio left hand $_T$ - rest), video Left (L) hand = (video left hand $_T$ - rest), audio False belief = (audio False belief story $_T$ - audio mechanical story $_T$), video False belief = (video False belief story $_T$ - video mechanical story $_T$), intentional triangles = (intentional triangles $_T$ - random triangles $_T$), vocalization = (vocalization $_T$ - non-human sounds $_T$), trustworthiness = (trustworthiness $_T$ - face gender $_T$), face gender = (face gender $_T$ - scrambled face $_T$), eyes intention = (eyes intention $_T$ - eyes gender $_T$), grasping = (grasping $_T$ - inclination $_T$), rotation = (hand rotation $_T$ - hand side $_T$) and saccades = (saccades $_T$ - rest). For each contrast, a map of statistical differences between tasks was estimated using a Student's t-test (t map).

In addition to SPM contrasts, individual conjunction maps were constructed to isolate voxels that were activated for multiple tasks (for instance to isolate the core system recruited across distinct modalities). These maps were created by taking the minimal t value of each of the contrasts considered for each voxel (Friston et al., 1999). In the results section, we used the term 'sentence' for the conjunction of 'audio & video sentences', 'right hand' for the conjunction of 'audio and video right hand', 'left hand' for the conjunction of 'audio and video left hand' and 'false belief story' for the conjunction of 'audio & video False belief stories'. Similarly, we generated individual exclusion maps, such as the 'trustworthiness without audio or video sentences' maps. In this example, we set to zero all voxels that passed the uncorrected p < 0.05 threshold (t > 1.64) for any of the audio or video sentence contrast. We used this liberal threshold to isolate at an individual level voxels which are likely to belong to one task correlate only and not the other ones, specifically when overlapping in a large extent.

2.6. Reliability of individual functional contrasts

We assessed the efficiency of our localizers to capture individual circuits using two approaches:

First, we evaluated the evolution of the signal-to-noise ratio within individual circuits throughout fMRI acquisitions, performing sub-analyses based on various numbers of trials, ranging from 2 to 8 or 10 depending on the total number of trials. For each SPM matrix, we calculated an individual average t value from voxels selected as follows: in an individual sub-contrast map, we only considered voxels that belonged to the final individual contrast threshold (at t > 2.33, p < 0.01 uncorrected – such liberal threshold was used considering the small number of trials) calculated on the maximal number of trials. To restrict focus on a specific circuit, we also intersected the resulting set of voxels with a group mask, calculated as the sum of thresholded (t > 2.33, p < 0.01 uncorrected) and binarised 78 individual corresponding contrast maps. This masking took into account the interindividual variability and was less strict than a random effect analysis. This analysis was performed for 2 to 3 representative contrasts of interest for each localizer.

Second, we took advantage of the test/re-test situation provided by the IBC dataset. Within-subject inter-sessions similarity was computed as the averaged correlation between all pairs of functional images available for a given contrast (3 pairs in the case of two sessions, 6 pairs in the case of four sessions). Inter-subject similarity was computed as the averaged correlation between all pairs of functional images available for a given contrast and different subjects. Inter-task similarity corresponds to the averaged correlation between all pairs of functional images from different contrasts. Images were masked by a volume representing the grey matter.

We also statistically assessed the intra-/inter-subject differences using a Multi-Dimensional Scaling (MDS) procedure. For a given task, we applied a three-dimensional principal component analysis (PCA) to all available functional contrast images across subjects and sessions (two or four per subject). This allows a visual representation and calculation of the inter-sessions within-subject distance in a reduced 3-dimensional space that captures the greatest proportion of variance. Within this 3-D space, we calculated for each subject i the averaged Euclidian distance D_i between his sessions (2 or 6 distances) for a given contrast. In the same way, we calculated the distance between all sessions associated to different subjects. We obtained 55 intra-subject and 1248 inter-subjects distances for the Pinel et al., 2007 and Parietal Localizers, 38 intra-subject and 592 inter-subjects distances for the Social Cognition and 13 intra-subject and 312 inter-subjects distances for the Social Face Localizers. For each contrast, we applied a non-parametric Wilcoxon signed rank test onto the intra- vs. inter-subject distances to test if intra-individual distances were shorter that the inter-subjects distances.

2.7. Group level analysis

To isolate at the group level the neural circuit evoked by each of our tasks, SPM voxel-based random effect analysis (RFX) were performed on the 78 individual smoothed contrast, conjunction and exclusion images (5 mm FWHM) at a voxelwise threshold of p < 0.05 corrected for multiple comparisons across the brain volume (Family-wise error correction based on random field). The RFX analysis provides robust results, taking into account the between-subject variability to estimate the group effect. To illustrate the cortical surface recruited by our localizers, we computed three-dimensional maps of activation and deactivation overlaps at the group level. The activation overlap map was obtained by performing one-sample tests across subjects for each of the 29 experimental conditions (task vs. rest), thresholding the result with a p < 0.05 corrected for multiple comparisons to obtain a binary map. We then summed these binary images to count how many times any given voxel was involved in significantly active regions. We replicated this for negative effects, using the same procedure on the negated maps (rest vs. task).

2.8. Subject level analysis

As our localizers were designed to isolate regions of interest (ROIs) at the individual level, we tested their robustness in 11 spherical ROIs of 5 mm radius (taken into account for interindividual variability). These ROI could be considered as important nodes, as they were located in a region where extended functional overlaps were noticed in the group analysis: STS/TPJ, mPFC, pCC, left frontal regions and intraparietal

sulcus. Similar analyses in two additional sites are reported in the supplementary materials for the right hemisphere). To calculate the position of a ROI's center, we averaged the coordinates of the nearest local maximas of all contrasts presenting an activation intersecting with the sphere at a corrected $p < 0.05$.

Because of the small number of trials performed in our protocol (10 trials max), we chose an uncorrected threshold $p < 0.01$, $t > 2.33$, for individual analyses. For each ROI and each contrast intersecting it at the group level, we reported the number of subjects who actually presented activation, as well as the average activation size (voxels number).

To find out whether the overlaps observed across conditions at the group level really reflect functional nodes or only results from image smoothing and intrasubject variability, we performed similar ROI-based analysis for each combination of the considered contrasts (using conjunction/exclusion maps). We reported the number of subjects was voxel passed the uncorrected threshold $p < 0.01$, $t > 2.33$. In contrast to the convergence issue, we roughly estimated the degree of voxel specificity in each ROI considering our limited set of tasks. We calculated the percentage of activated voxels that passed the $p < 0.01$ threshold in one contrast only (having a p value > 0.01, meaning no significant, in other contrasts), two contrasts only, three contrasts only and so on. Because some voxels were not selected by any of these categories, the total of reported amounts was sometimes less than 100%.

2.9. Neurosynth meta-analyses

In order to further establish the validity of our protocol, we tested whether the patterns of activity found in our study at the group level replicated previous findings. Therefore, we performed a series of meta-analyses using the Neurosynth automated analysis system (Yarkoni et al., 2011). We selected terms of interest related to our protocol in the Neurosynth database. Neurosynth generates z-scores maps (called here uniformity test map) derived from a one-way ANOVA, testing whether a voxel is consistently activated in the studies tagged with the term of interest. These maps are automatically thresholded to correct for multiple comparisons (False discovery rate $= 0.01$). We downloaded maps associated to the following terms (indicated with quotation marks for avoiding confusion with ARCHI contrast names) in relation to our protocol: 'Social cognition' (220 studies selected), 'Mind ToM (74 studies), 'Mental states' (118 studies), 'Gaze' (117 studies), 'Intentions' (125 studies), 'Emotional stimuli' (212 studies), 'Others' (58 studies), 'Face' (896 studies), 'Reading' (521 studies), 'Speech perception' (97 studies), 'Language comprehension' (107 studies), 'Calculation' (76 studies), 'Saccades' (73 studies), 'Grasping' (90 studies), 'Object' (851 studies), 'Visuospatial' (267 studies), 'Rotation' (102 studies), 'Motion' (451 studies), 'Hand' (879 studies), 'Action' (634 studies), 'Movement' (670 studies) (the database was accessed at http://neurosynth.org/analyses/terms, except for the term 'Others' which required a customized analysis available on http://old.neurosynth.org/analyses/custom). Maps were resampled to match the resolution of the ARCHI contrast images (3 × 3x3 mm).

We examined 12 of our contrasts of interest: False belief, trustworthiness, intentional triangles, eyes intentions, face gender, video sentences, audio sentences, vocalization, calculation, saccades, grasping and rotation contrasts. We also considered an additional contrast to summarize activation evoked by hand actions: hand movement $=$ (audio right hand $_T$ + video right hand $_T$ + audio left hand $_T$ + video left hand $_T$ − audio calculation $_T$ + video calculation $_T$ - audio sentence $_T$ - video sentence $_T$). We then generated a matrix of similarity, calculating for each pair of ARCHI and Neurosynth contrast a correlation coefficient.

3. Results

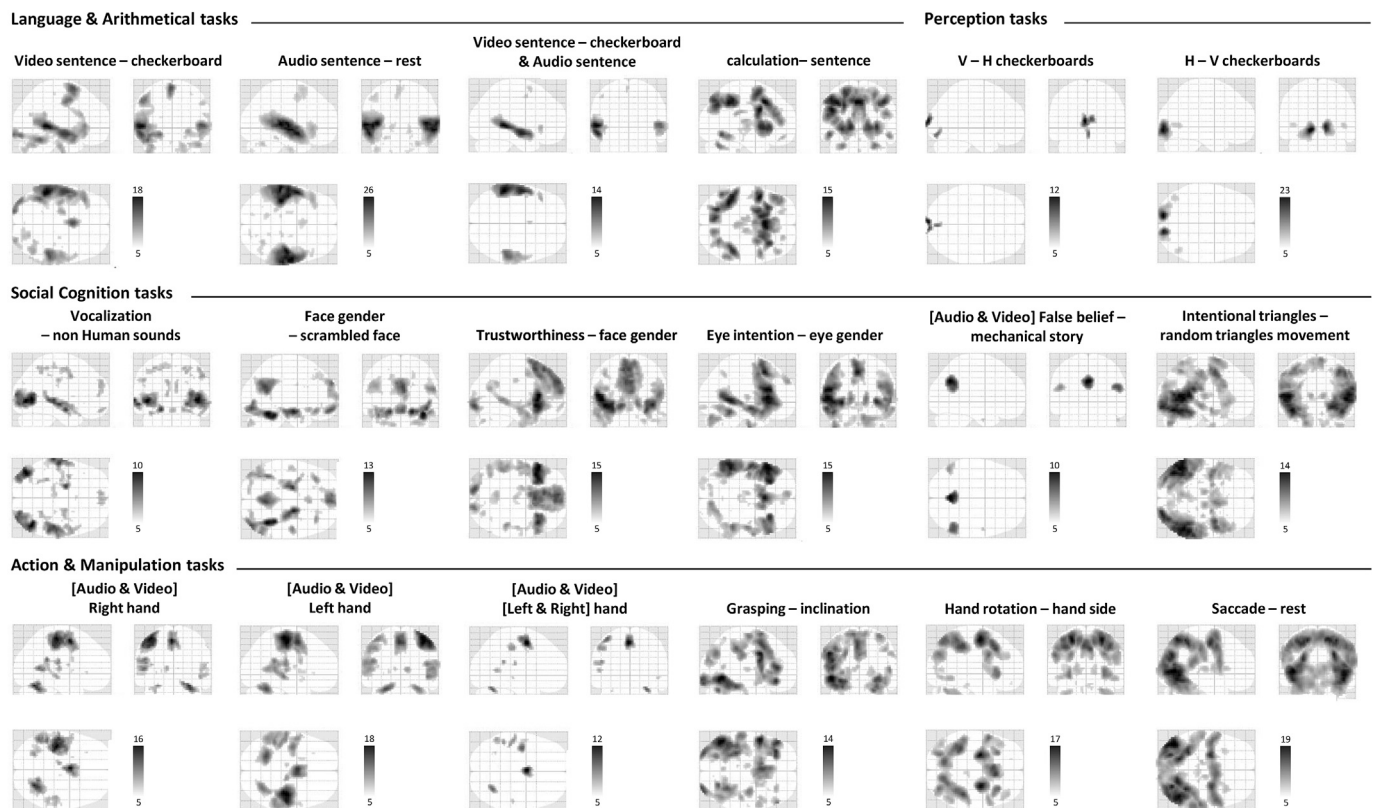We displayed in Fig. 1 standard SPM random effect (RFX) group

Fig. 1. Three dimensional SPM glass brain projections of group analyses. For each contrasts of interest, we plotted sagittal, axial and coronal views of the RFX analysis performed on 78 subjects (77 subjects for the face gender, face trustworthiness and eyes intention task). All voxels passed a $p < 0.05$ significance ($t = 5.34$), corrected for multiple comparisons.

analyses performed on the individual contrasts of interest and projected on the three directions of transparent brains. A detailed and complete listing of all the main foci of activation is reported in the Supplementary Table 1. To further appreciate the functional covering of medial, temporal and dorsal regions, we grouped these contrasts in three different generic cognitive domains: "symbol manipulation" for word and number encoding, manipulation and representation; "social cognition" for tasks that require understanding other's intention, mental state or belief; "motor or visuospatial" for preparation and execution of eyes or hand movement and internal manipulation of visual objects. These domains are plotted on an individual anatomy Fig. 2. Isolines allowed a clear visualization of the maps' extensions, as well as the organization of their respective peaks.

As it could be seen on Fig. 1, both the audio and video sentence tasks evoked left lateralized perisylvian circuits composed of activations within the left inferior-frontal gyrus and bilaterally along the STS. Depending on modality, additional activity within the left ventral visual pathway (which matches the reported location of the VWFA) was reported in the case of visually presented sentences or in Heschl gyrus for auditory presented ones. The calculation contrast showed a large bilateral network, composed of activations in left and right IPS and posterior superior parietal lobes (PSPL), the supplementary motor area (SMA) and the mPFC, the frontal eye fields (FEF), the precentral gyrus (PG), the putamen, the thalami and the cerebellum. Consistent with our previous study based on this localizer, we used the main effect contrast (Pinel et al., 2007). Conjunction across modalities resulted in less extended activities, but roughly maintained the same circuit (see Supplementary

Fig. 4 for comparison). Areas activated by the Checkerboard contrasts roughly mapped the primary and extrastriate visual areas. The vertical vs. horizontal contrast showed activation of the V1/V2 ventral and dorsal borders, while the horizontal vs. vertical contrast revealed left and right visual areas in V1 and in the occipitotemporal gyri. The vocalization contrast isolated activation of the left and right superior/middle temporal cortices, left hippocampus and right amygdala. Additional unexpected activity was found essentially in the posterior middle temporal gyrus (mTG) and, to a lesser extent, beside the FEF and in the superior parietal cortex. Checking activation of the non-human sounds trials versus rest showed that this posterior cluster was not due to a deactivation during the control task. The face gender contrast isolated bilateral lateral occipital areas and inferotemporal cortex, with a noticeably strong right lateralized activation of the fusiform face are (FFA). Activity was also found in various parts of the limbic system (i.e. OFC, left and right hippocampus, and right amygdala), the rostral medial frontal cortex, the precuneus/pCC and bilateral foci in the TPJ and the anterior mTG. The trustworthiness contrast showed a bilateral circuit encompassing part of the frontal lobe (large activation along the mFG up to the preSMA, inferior frontal areas/insula). Further activity was found in the pCC, lingual gyri, STS and right cerebellum, and, in the left hemisphere only, in the TPJ and in the dorsolateral frontal cortex. In subcortical nuclei, we found recruitment of the thalamus, putamen and palidum. The eyes intention contrast showed similarities with the pattern and asymmetry of the reading contrast: strong activation along the left and right STS, inferior frontal area and insula, precentral areas and within the left inferotemporal visual areas. We also found a spot of activity bilaterally in
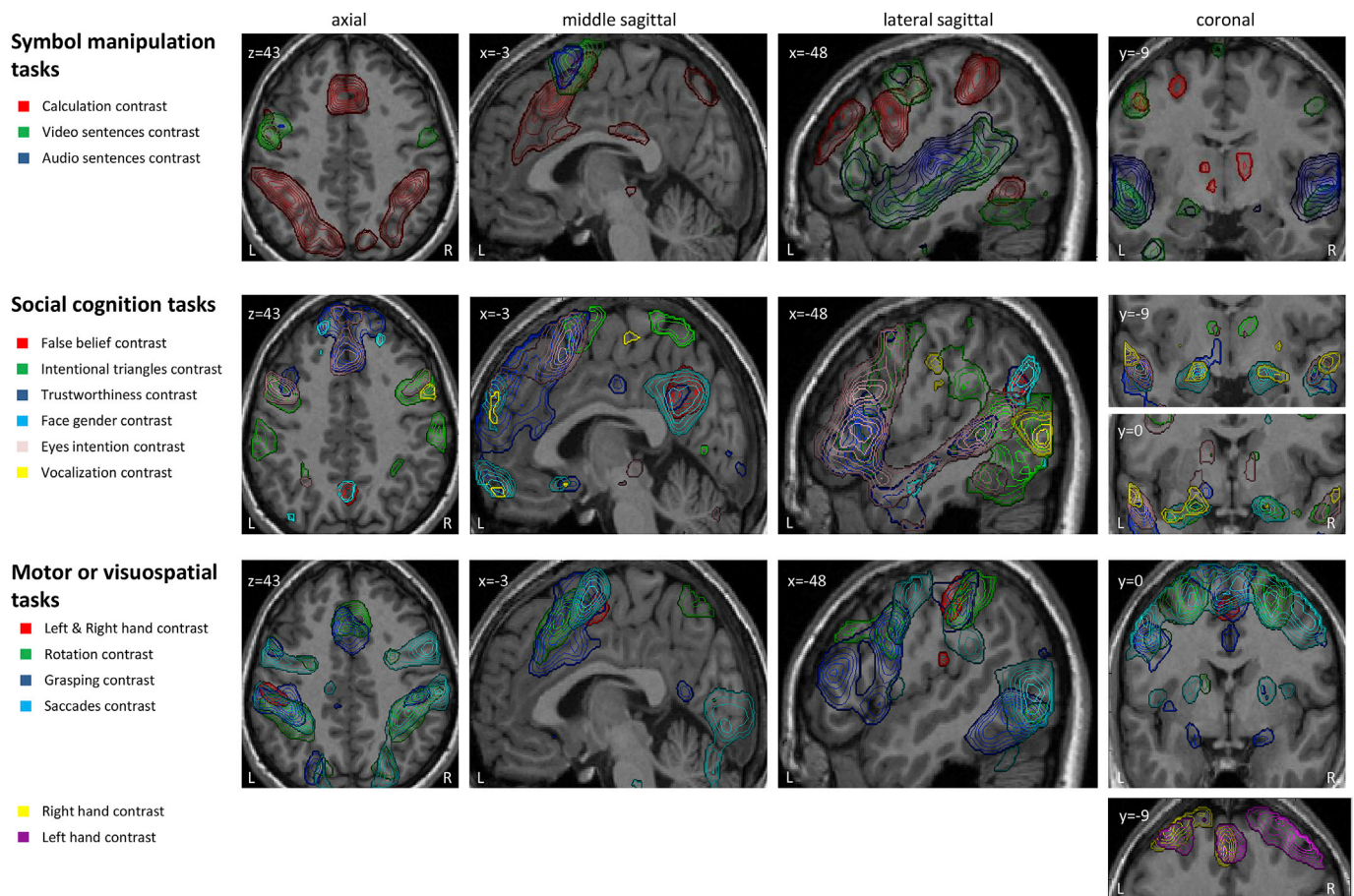

Fig. 2. Anatomical projections of contrasts of interest. Here we detailed cortical regions activated in our study (RFX group analysis) within the intraparietal parietal cortex, medial areas, left lateral frontal and temporal lobes, subcortical nuclei and motor cortex (Neurological convention). Activations are plotted as isoline, each line representing constant t value. This allows seeing extension as well as local peaks of overlapping contrasts (see contrast definitions in material and methods part). L = left hemisphere, R = right hemisphere.

the cerebellum, thalami and caudate nuclei. The conjunction of audio and video false belief contrasts showed a remarkably restricted circuit, including essentially the bilateral TPJ and the precuneus/pCC region. The main effect of false belief versus mechanical story independently of the modality showed a larger network including in addition the mPFC and the STS bilaterally (see Supplementary Fig. 4). However, by discarding activity related to visual and auditory modalities, the conjunction provides a more specific access to the core brain system of ToM. The intentional triangles contrast showed an extended bilateral activation of extrastriate visual areas up to MT/V5 and extrastriate body area (EBA) regions, occipitotemporal gyri, cerebellum, supramarginal areas, superior parietal (including the anterior intraparietal - AIP) and postcentral cortices. Bilateral activations of the PG, the FEF, the SMA and the inferior frontal areas were found in the frontal lobe, as well as subcortical activation (i.e. bilateral thalami, right amygdala and putamen). Conjunction of audio and video right hand action tasks revealed an amodal circuit including left primary motor and somatosensory cortex, rolandic operculum, SMA and right cerebellum. The left hand action task activated the right primary motor and somatosensory cortex, the left and right rolandic operculum, the SMA, the left cerebellum and part of the left postcentral gyrus (pCG) and premotor cortex. The conjunction across hand and modalities showed a small motor circuit, mostly restricted to the SMA and left rolandic operculum, precentral and postcentral cortices. The grasping contrast revealed a strong activation of the lateral occipital (LO)

area, the precentral gyrus, postcentral gyrus/anterior IPS, motor cortex, mPFC, SMA, preSMA, dorsal anterior cingulate cortex (dACC), inferior frontal area and ventral medial frontal gyrus. Additional activity was observed in the occipitotemporal lobes and subcortical nuclei (thalamus, putamen and amygdala). Most of these activations presented a leftward asymmetry, particularly, in the mTG, frontal and parietal cortices. The rotation contrast activated a bilateral superior frontal gyrus and the preSMA. Superior parietal activations extended from the pCG to the PSPL and superior occipital gyrus (SOG). Additional activity was found bilaterally in the caudate nuclei, the insula and in the cerebellum, as well as the left temporal lobe in the vicinity of the EBA. The saccades task activated bilaterally the primary motor cortices (BA 4), the SMA, superior frontal cortex at the FEF sites, pCG, IPS, PSPL and SOG. Large activations were isolated in the visual areas, MT/V5, and inferotemporal cortex, subcortical nuclei (putamen, thalami), insula and cerebellum.

As a whole, neural territories recruited by our localizers covered most of the cerebral cortex (Supplementary Fig. 5). When considering activation from all the 29 experimental conditions, we calculated that 82% of voxels showed a positive suprathreshold activity in at least one of the condition, with the exception of the most anterior part of the frontal and the inferotemporal lobes. However, when considering the 29 rest vs. condition contrasts, we found that 84% of voxels showed a negative suprathreshold activity in at least one of the contrasts. This included maximal overlaps in the precuneus and the posterior cingulate cortex, the
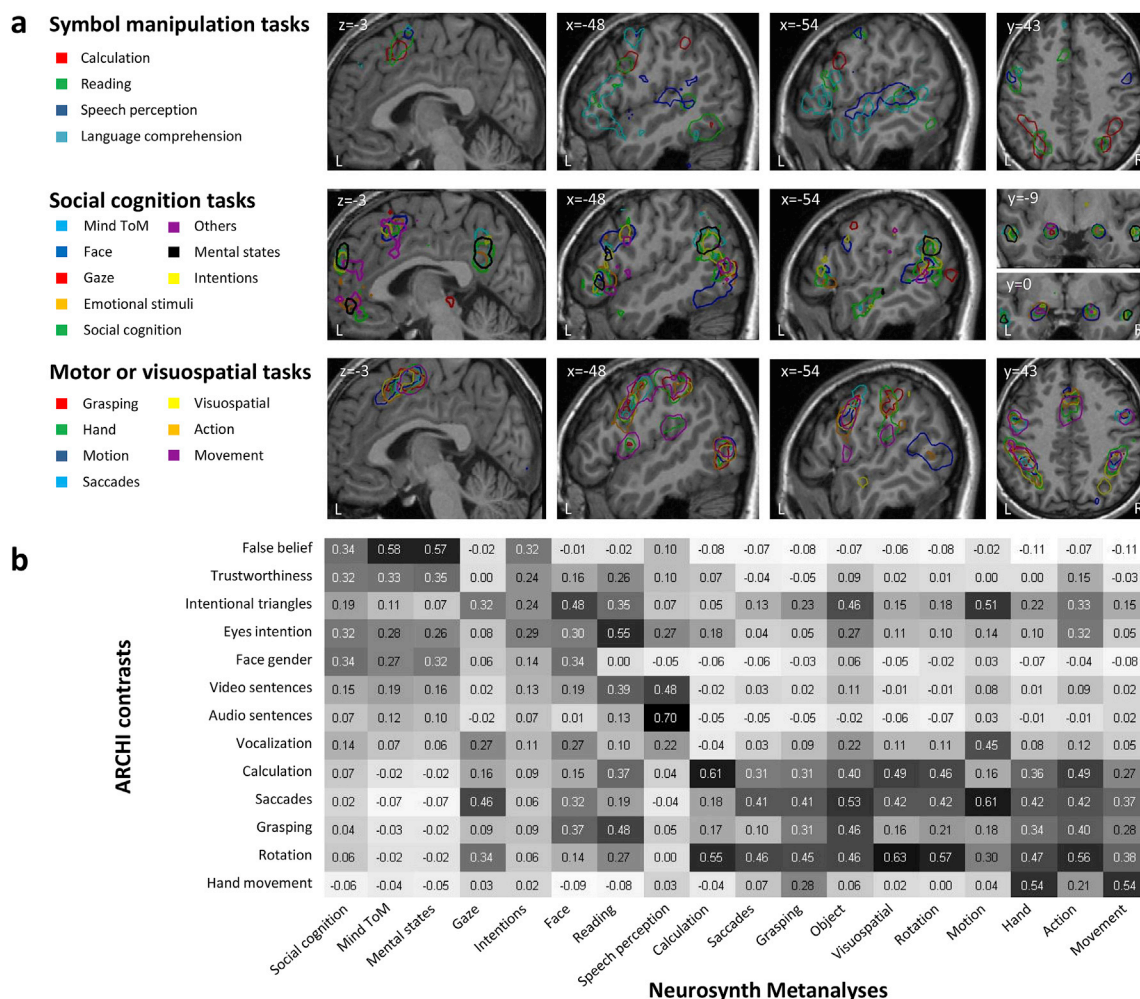

Fig. 3. Comparison with Neurosynth meta-analyses functional maps. (a) Anatomical projections of Neurosynth meta-analyses. Here we detailed cortical regions displayed in Fig. 2 for comparison with our localizers' results: the intraparietal parietal cortex, medial areas, left lateral frontal and temporal lobes and subcortical nuclei (Neurological convention). Terms used for meta-analysis are displayed on the left. L = left hemisphere, R = right hemisphere. (b) Correlation matrix between 13 ARCHI functional maps (vertical axis) computed from the group analyses and 18 Neurosynth meta-analyses based on terms displayed on the horizontal axis.

angular gyrus and the medial prefrontal and orbitofrontal cortex which are generally encompassed in the default mode network (Raichle et al., 2001).

To assess the consistence of our results with those reported in the literature, we performed a series of meta-analyses on the Neurosynth database of published functional maps (Fig. 3a). The patterns acquired through ours tasks shown a similar disposition to the meta-analysis ones in each cognitive domain. A matrix of similarity performed between 13 of our contrasts of interest and 18 functional patterns derived from Neurosynth meta-analyses is plotted on Fig. 3b. To facilitate reading, images names have been placed in comparable semantic order on the vertical and horizontal axis. Various contrasts preferentially matched with their Neurosynth counterparts: we found high correlation coefficients (c) between false belief and 'Mind ToM' ($c = 0.58$) and between false belief and 'mental states' ($c = 0.57$); between trustworthiness and 'social cognition' ($c = 0.32$), 'Mind ToM' ($c = 0.33$), and 'Mental states' ($c = 0.35$); between face gender and 'face' ($c = 0.34$), and 'social cognition' ($c = 0.34$); between video sentences and 'speech perception' ($c = 0.48$), and 'reading' ($c = 0.39$); Between audio sentences and 'speech perception' ($c = 0.70$). Between calculation and 'calculation' ($c = 0.61$); between saccades and 'saccades' ($c = 0.41$), 'gaze' ($c = 0.46$), 'motion' ($c = 0.61$), and 'visuospatial' ($c = 0.42$); between rotation and 'rotation' ($c = 0.57$), and 'visuospatial' ($c = 0.63$); between hand movement and 'hand' ($c = 0.54$), and 'movement' ($c = 0.54$). Other contrasts presented coherent but more complex and less specific profiles but overall, the similarity matrix is organized along a diagonal axis (e.g. grasping correlates with 'grasping' ($c = 0.31$), 'object' ($c = 0.46$), 'hand' ($c = 0.34$) and 'action' ($c = 0.40$), but also with 'face' ($c = 0.37$) and 'reading' ($c = 0.48$)). Some inter-domains correlation could be noticed: calculation showed additional strong correlation with 'rotation' ($c = 0.46$) and saccades ($c = 0.49$), eyes intention was correlated with 'reading' ($c = 0.55$), while it correlated also with 'face' ($c = 0.30$) and 'social cognition' ($c = 0.32$), intentional triangles correlated with 'face' ($c = 0.48$), 'motion' ($c = 0.51$), 'object' ($c = 0.46$) and 'reading' ($c = 0.35$) and vocalization with 'motion' ($c = 0.45$) and, in a lesser extent, with 'face' ($c = 0.27$).

In some of the experimental conditions, correlations might have been lowered by differences of extent between our contrasts and meta-analyses from Neurosynth. For instance, small activation clusters, specific to a particular experimental design in the literature may have disappeared or been smoothed in a larger network based on a meta-analysis.

In an anatomo-functional perspective, we examined to what extent we replicated the shape, location and geometry of patterns reported in the literature. For simplification we limited here our comparison between Neurosynth and ARCHI to the views displayed Fig. 2 considering three distinct cognitive domains. The functional organizations displayed in Fig. 3 on the three medial/frontal views were virtually identical to those from ARCHI (Fig. 2).

On the middle sagittal view, various activations were found intermixed near the SMA/preSMA area for the symbol manipulation and the motor and visuospatial tasks in both figures. By contrast, four distinct areas are clearly identified for the social cognition tasks: the OFC, the mPFC, the preSMA/anterior cingulate cortex (aCC) and the pCC/precuneus. Our social tasks specifically allowed to isolate these medial regions. Two additional areas were reported in our localizer: within the ventromedial prefrontal cortex, where face gender, vocalization and trustworthiness contrasts showed activation, and in the precuneus for the intentional triangle contrast.

On the sagittal views, two prefrontal and precentral, one intraparietal and one inferotemporal areas can be noticed for the calculation contrast. All of them could be seen at identical locations in the 'calculation' meta-analysis, except the more anterior prefrontal one, that could be seen in a more median slice ($y = -44$). The left frontal and perisylvian network built from the 'language comprehension' meta-analysis was replicated here with our video sentence contrast. Concerning the preservation of the geometrical details of this pattern, we could notice similar posterior mid-

temporal activation from video sentence contrast and 'reading' meta-analysis, an extended activation common to both modalities (see conjunction Fig. 1) and to 'language comprehension' meta-analysis, and superior temporal activation for the audio modality and 'speech perception' meta-analysis. Interestingly, the precentral gyrus appeared to host a more posterior site for language (shared by video sentence – Fig. 2, 'reading' and 'language perception' – Fig. 3) and one more anterior for calculation (contrast and 'calculation' meta-analysis). Inferotemporal activation associated to video sentence contrast and 'reading' meta-analysis were found in both analyses, restricted to the video modality. In the meta-analyses based on social cognition terms, we found three main areas. A large one within the posterior temporal lobe, extended vertically from the inferotemporal gyrus up to the TPJ, activations along the anterior STS and two inferior and middle frontal sites. We found a covering of the temporal and frontal cortices very similar to the one observed with our social cognition tasks. The TPJ isolated with the 'mind ToM and 'mental states' fully overlaps with our activation from the false belief contrast. Slightly more anteriorly, a spot isolated with 'intentions' matches with the STS location of the intentional triangles contrast. In the middle part of the STS was found activation for the 'face' meta-analysis, than may be spatially related to the face processing involved in the trustworthiness and eyes intention tasks. Only the intentional triangles contrast exceeds these boundaries into the direction of the inferior parietal/postcentral region. Different properties of the anterior and posterior sites are further discussed in Fig. 5 in light of the result of the ARCHI database. Meta-analysis based on motor or visuospatial terms isolated a set of areas covering the precentral and postcentral gyri, iFG, occipito-temporal region and rolandic operculum. This finding fits our tasks involving visuospatial processing or action preparation, except the grasping task that revealed an extended activation within the mPFC.

Last, on the axial view, we observed similar frontoparietal networks in both analyses (Figs. 2 and 3). The main difference is the presence of clusters for the 'reading' Neurosynth analysis, in the IPS. The bilateral IPS supports activation associated to 'calculation'. More anteriorly, we see a leftward recruitment of the IPS for 'grasping', 'hand' and 'action' related studies, while more posterior parietal sites are associated with visuospatial, motion and grasping (convergence is not seen here but apparent at $z = 38$). This echoes the leftward activation of the anterior IPS/AIP found for the left & light hand contrast and the grasping contrast, while posterior areas are more involved in mental rotation and saccades task, implying various visuospatial functions. Two coronal views underlined the importance of subcortical nuclei for social task, that where activated bilaterally in the same extent for ARCHI meta-analysis and for our social cognition tasks.

As seen on Fig. 2, some brain regions support complex and intermixed patterns of activity for different functional contrasts. These different tasks activated, at least at the group level, either complementary or convergent areas. For instance, sentences and social cognition tasks recruited overlapping sites along the STS, while some of the social cognition and visuospatial tasks presented activation in the posterior mTG. Altogether, these activations cover the temporal lobe with an apparent anteroposterior organization. Similar observation could be made in the middle sagittal view. Motor and visuospatial tasks present a clear overlap with sentences and calculation tasks posteriorly, but also with social cognition tasks, which spread more anteriorly to the OFC. To describe such a mosaic in more details, we presented on Fig. 4 activation patterns resulting from distinct contrasts or contrasts combinations (conjunction or exclusion maps) which presented activated voxels within the left temporal lobe. The isoline representation allows visualizing and comparing the core structure (peaks) of close or convergent circuits. The entire length of the STS was illustrated here in various functional combinations, and some nodes could be identified.

In the most anterior part of the STS, we found a convergence of language (audio and video sentences) and social tasks (intentional triangles, eyes intentions and trustworthiness tasks). In a more posterior part of the STS, was functionally subdivided in three distinct zones: one is identified
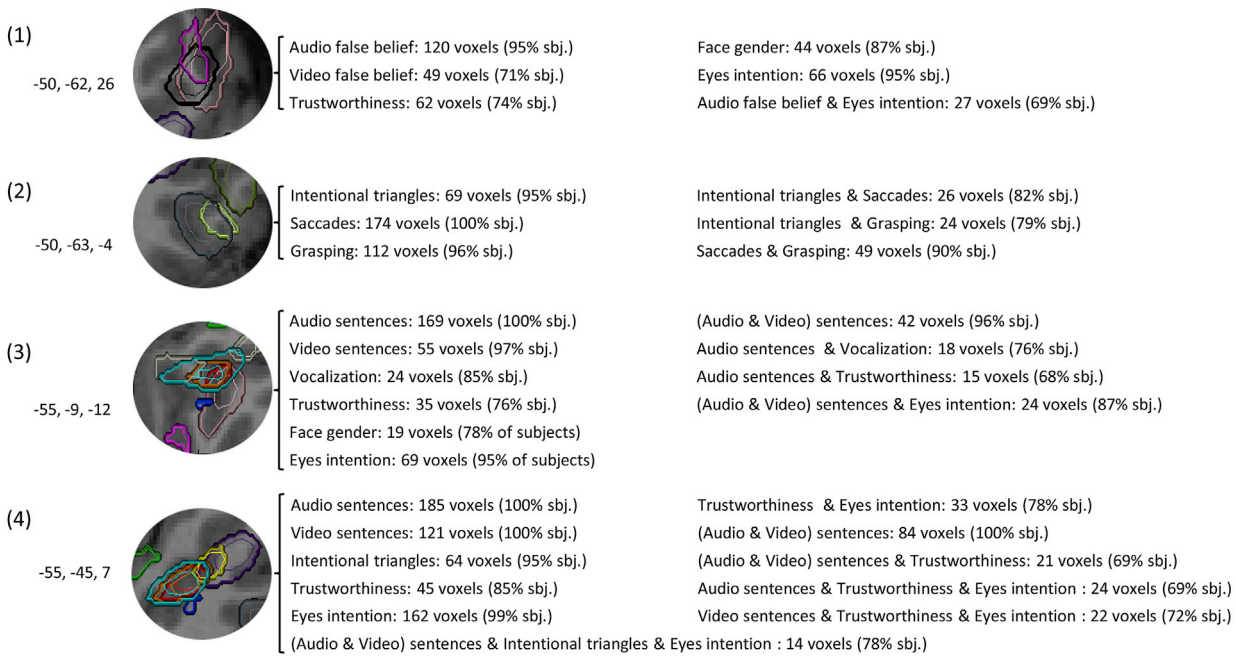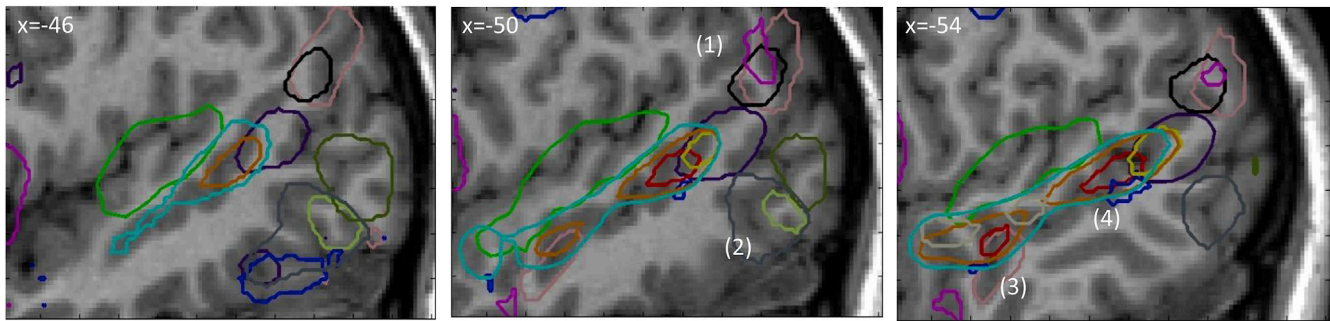
Fig. 4. Functional mosaic of the left temporal lobe. We projected on three sagittal slices cortical territories isolated in our functional contrasts and covering the temporal lobe (Labels correspond to the contrasts' names are described in Material and methods, 2.4. '&' refers to a conjunction and 'without' to an exclusion). Activation patterns are delineated with t value isolines corresponding to $t = 5.19$ ($p < 0.05$ corrected for multiple comparison). In order to make the figures clearer, we sometimes grouped activations as conjunction when the overlap of their activation was similar as their respective extents. Notably, this helps to see functional nodes present along the superior temporal sulcus. For four areas of important functional overlapping, we display detailed view of the activation peak locations (plotting more isoline but selecting the 30% highest t values only for each contrast) inside a spherical ROI. For each ROI are reported frequency (in % of subjects) and average size (in voxels) of individual activation and conjunction that could be reported for at least 2/3 of subjects. (sbj. = subjects, R = Right, L = left, & = conjunction).

by the conjunction of sentences and trustworthiness contrasts, a more posterior one is identified by sentences, intentional triangles and eyes intentions contrasts, and a third one by intentional triangles and eyes intention only. Last, the most posterior part of the STS, extending to the TPJ presented an overlap between the trustworthiness contrast (once we excluded all language activation), the gender face and the false belief tasks. Below the STS activation, the functional mosaic is completed with various combinations of grasping, saccade, vocalization and intentional triangles contrasts. Note that this allowed, for instance, splitting the intentional triangles contrast into a superior temporal part, shared with eyes intention contrast and so more dedicated to the analysis of other's intention, and a more inferior mTG one, shared with saccades and grasping, and more likely involved in the more general attentional orientation.

Considering that group analyses are just a raw method to approach a

refined understanding of the cortical organization, we examined the relevance of these activations and conjunctions at the individual level. In four regions of high functional convergence, we calculated the proportion of participants whose activity was significant at the uncorrected voxel p-value < 0.01. We only reported it when it was greater than a representative proportion of subjects (two-thirds of subjects - 66%) (Figs. 4 and 5). This arbitrary threshold was used to illustrate activations that can be expected at the single subject level using our localizers. Strikingly, most of the activations and contrasts conjunctions reported at the group level could also be reported at the individual level. Specifically, in the node (4) of Fig. 4, the audio and video sentences, the intention triangles and the eyes intentions contrasts partially shared the same voxels in 78% of individuals, suggesting a genuine functional convergence at the single subject level. More generally, in region (4) 49.6% of voxels were activated by one task only, 24.5% by two tasks, 14.7% by
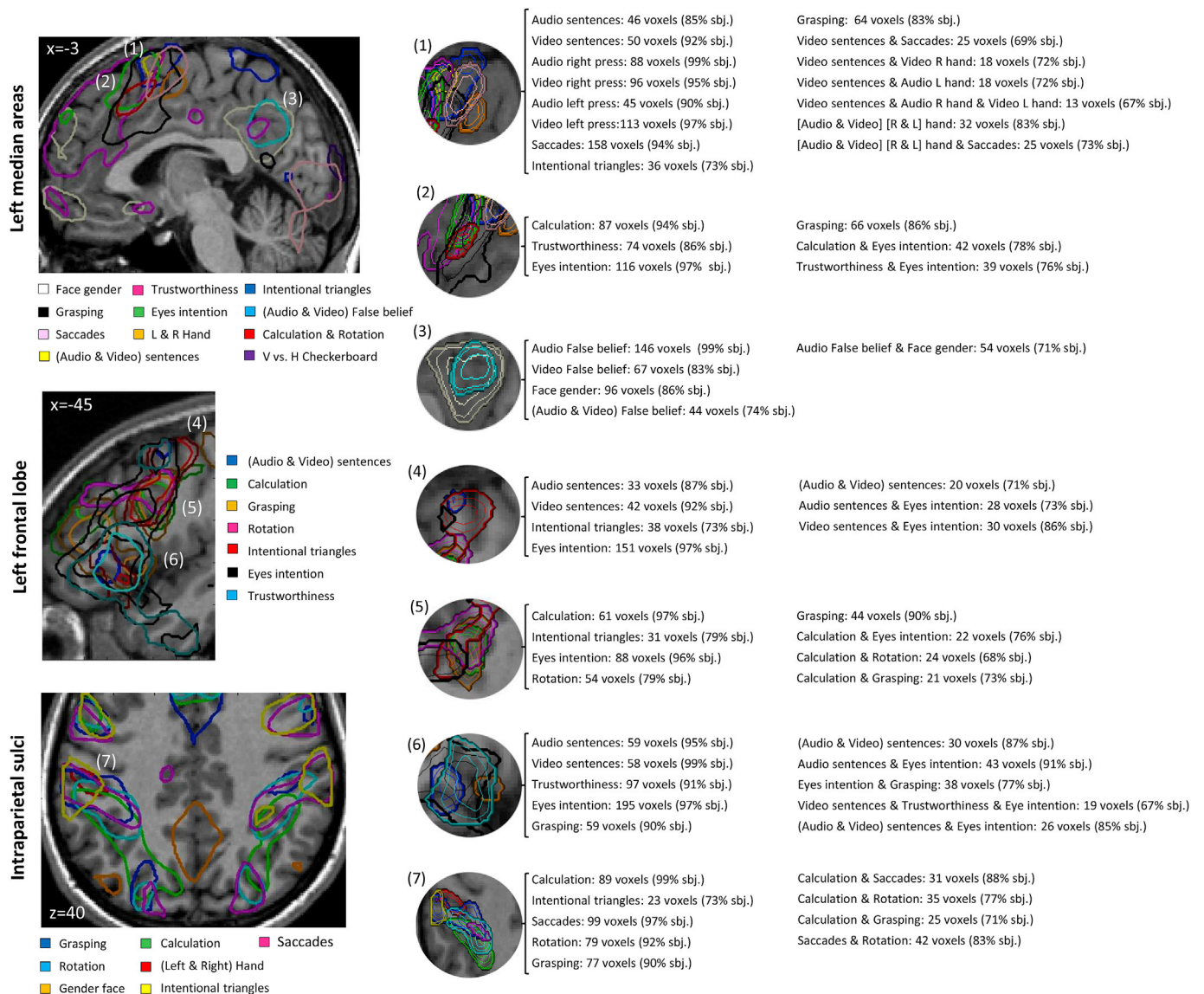
Fig. 5. Functional mosaic in the left median, left frontal and superior parietal regions. See caption of Fig. 3 for details. Coordinates (x, y, z) of the selected ROIS (1–7) are [-3 6 66], [-3 17 47], [-3 -49 35], [-45 11 28], [−45 3 49], [-45 24 2] and [-48 -41 40], respectively (L = left, R = right).

three tasks and 5.2% by four tasks. As a whole, voxels of this region have the highest redundancy across the tasks of our protocol. In region (3), 64.7% were activated by one task only, 18.7% by two and 5.6% by three tasks. More ventrally, in region (2), 66.7% were activated by one task only, 26.2% by two and 3.4% by three tasks. Finally, the TPJ region (1) has the lowest level of multi-domain voxels: 72.1% were activated by one task only and 10.6% by two tasks, suggesting the presence of three close but distinct sub-areas. Comparatively, the right STS presented a strikingly different profile, with less regions of multi-tasks convergence (see Supplementary Fig. 6). At the individual level, we did not find more than two tasks sharing same cluster of voxels in a substantial number of participants. A majority of individuals' voxels in the STS showing the maximal contrasts overlap were activated by one task only (70.2%), and the other ones (13.8%) no more than two tasks. Interestingly, the highly consistent individual conjunction between audio and visual false belief contrasts found in the right TPJ was not present on the left side.

The same type of description and analysis was conducted for the medial areas, the left frontal lobe and the superior parietal lobe (Fig. 5). Some cortical regions are almost totally covered, such as the middle frontal gyrus and the left frontal cortex. A high density of overlap could be observed in the preSMA/SMA areas, the left inferior frontal region in the vicinity of Broca areas and in the left AIP. Indeed, Region (1) showed a particularly high amount of overlap at the individual level for motor contrasts, and the preSMA various overlaps between motor, social and calculation contrasts. Again, note that in some cases, as in the precentral region (5), the absence of shared voxels in any conjunction at the individual level suggests that this area likely supports separate clusters, even if overlaps were observed at the group level. The IPS showed a high level of conjunction in its anterior part (7) between the calculation and visuomotor tasks (grasping, saccades and rotation task).

Fig. 6.a shows that after 8–10 trials, most of the individual functional contrasts of interest, if not all, passed a p < 0.01 uncorrected threshold (t > 2.33) to reach in some cases a p < 0.001 threshold, suggesting that all tasks were correctly performed by 100% of our subjects. These thresholds are relatively liberal but relevant, considering the small number of trials performed in our design. Distributions of the individual averaged t maps for the ten selected contrasts presented similar logarithmic evolutions with a trial number, and a reduction of the inter-subjects variance, suggesting that all subjects performed the experiment in a similar efficient way (in term of attention paid to the tasks) with virtually almost no outlier. To test whether functional contrasts were specific, to some extent, to individuals, we computed the
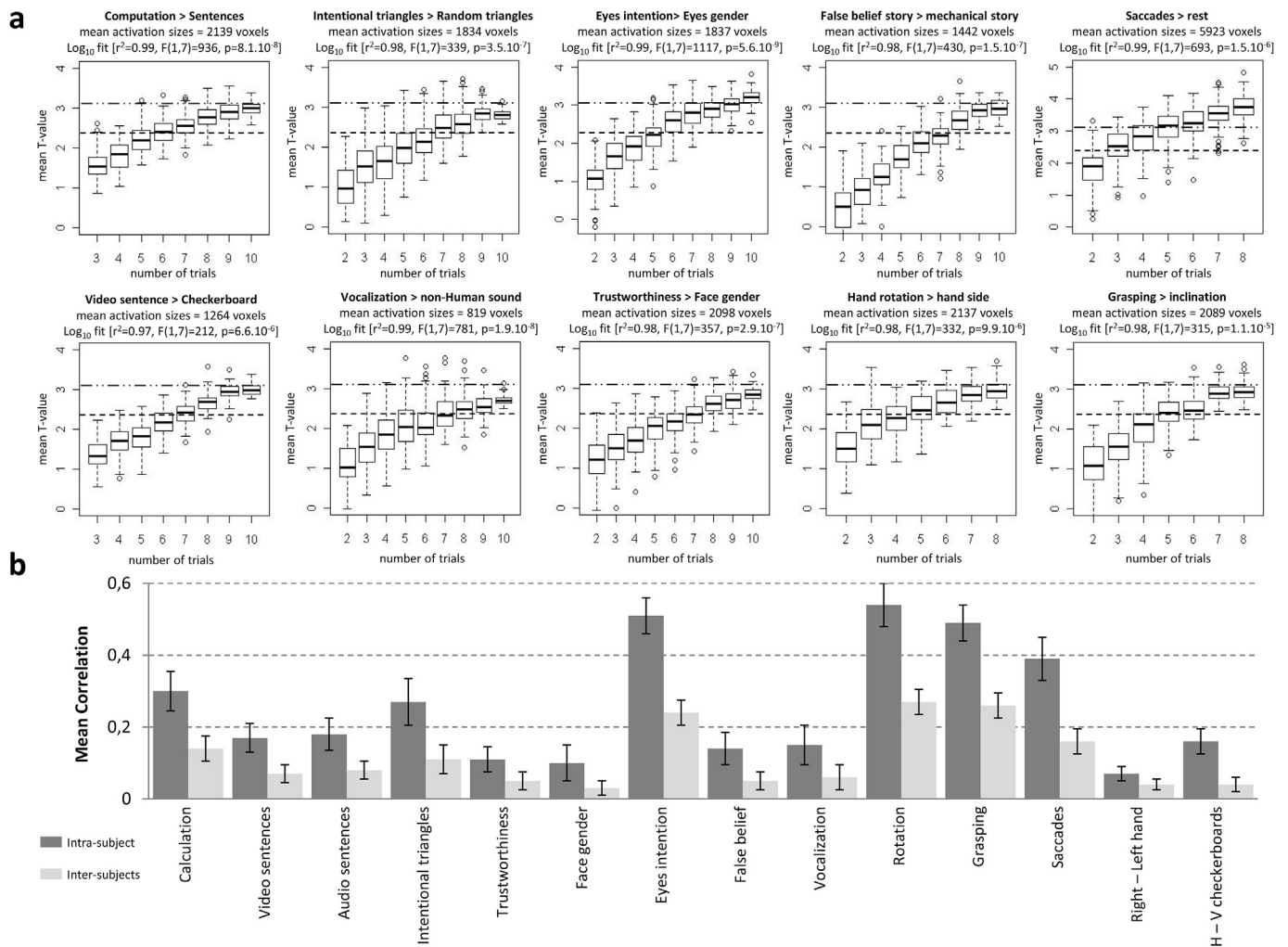
Fig. 6. Efficiency of the ARCHI protocols to capture individual patterns. (a) Evolution of mean t values of individual activations with number of trials. For main contrasts of interest, we display how the averaged t value over activated voxels increases throughout scanning. For each additional trial, boxplots show the median of individual average t values, upper and lower quartile, as well as the extreme range of values excluding outliers. Dots correspond to outlier. Mean activation size corresponds to the average of individual masks size used in voxels selection (see methods), and reported significance corresponds to a logarithmic fit of data (Log10 fit). The inferior dashed line corresponds to the T value associated to a p < 0.01 uncorrected threshold, and the superior one to a p < 0.01 uncorrected threshold. (b) Correlation between within-subject and inter-subjects session performed on the IBC dataset. Intra-subjects correlations (in dark grey) were calculated for all pairs of [session x phase encoding] combinations available for each subject, and then averaged across subjects (see Materials & methods). Inter-subjects correlations were calculated for all pairs of sessions belonging to two different individuals, and then averaged. Error bar = ± ½. $\frac{\sqrt{\sigma}}{\sqrt{N}}$ where σ is the variance and N the number of correlation values.

correlation values between within-subjects sessions from the IBC dataset, and compared them to the correlation obtained from all pairs of inter-subjects' sessions. In all tasks, averaged within-subject correlation values were superior to the inter-subjects ones. Another way to estimate the within-subject similarity was to calculate the inter-sessions within-subject distances and compare them to the inter-sessions inter-subjects distances, after reduction to a 3-D space with a PCA. P values of the Wilcoxon signed rank test for the difference between intra and inter-subjects distances were the following: 2.10^{-16} for calculation, 3.10^{-3} for video sentences, 3.10^{-3} for audio sentences, 3.10^{-3} for intentional triangles, 0.017 for trustworthiness, 0.013 for face gender, 2.10^{-5} for eyes intention, 3.10^{-5} for false belief, 3.10^{-5} for vocalization, 2.10^{-16} for rotation, 2.10^{-16} for grasping, 2.10^{-16} for saccade, 3.10^{-3} for right – left hand (= left – right hand p value by definition) and 5.10^{-13} for H – V checkerboards (= V – R checkerboards). This significant differences mirror 3-D plots displayed on Supplementary Fig. 7. For each contrast, most of the sessions performed by a given subject appeared grouped in the sessions' dots cloud (Distribution of the intra-subject: mean = 55,

lower quartile = 67; upper quartile = 82; Distribution for inter-subjects distances; mean = 109, lower quartile = 95; upper quartile = 122). The discriminability of individual patterns mostly depends on the disparity of neural response among the group as within-subject distance is quite stable among condition. Subjects' clusters appeared clearer when dots were more widely distributed, as was the case for the eye intention or the saccades contrast, while all sessions are more grouped together, for instance for visual or hand action contrasts. Testing across contrasts correlation between the mean activation extent (t > 2.33) and the mean inter-subject sessions' distances, we found a positive coefficient of 0.77 (p = 0.007), while mean intra-subject sessions' distances did not correlate significantly (c = 0.118, p = 0.69).

Finally, on Supplementary Fig. 8, we reported individual activity maps of four representative subjects (limited, for clarity, to 7 contrasts). This figure illustrates both the robustness of our contrasts at the subject level and the complexity of individual functional mosaics. For instance, we could observe intermixed activation of video sentence, eyes intentions and trustworthiness contrasts in the middle part of the STS. In

the TPJ, the cluster associated with trustworthiness was repeatedly found beside a cluster associated with the false belief and face gender contrasts. However, if the antero-posterior functional distribution along the STS shows a relatively similar organization across individuals, the number of clusters or the extension of a given contrast may vary significantly at the local scale.

4. Discussion and potential of the database

The present paper described the functional part of the ARCHI database, developed in the context of the CONNECT project (Assaf et al., 2013). With the Human Connectome Project, our database is a tentative to provide stimulating material comprising of a large collection of structural and functional images at the individual level. Our challenge was to design short localizers that are able to isolate, with a limited number of trials, a large range of functional networks, and to cover most of the cortical surface with a finer grain on specific regions of interest for the teams involved in the project (parietal cortex, temporal lobes and inferior frontal regions). Preliminary results from group analysis performed on 78 subjects showed that we successfully isolated several important regions for language, mathematics, social, motor, and visuospatial domains. These first maps shed light on the functional organization of the frontal, parietal and temporal lobes, and provide a new across-tasks description of the regions associated with a high-level of functional overlapping. Even though the combination of experimental conditions, brain regions, and type of analysis make it difficult to summarize here the globality of the potential results, we would like to suggest some directions for future exploitations of the database and use of the developed protocols.

In the temporal lobe, the anteroposterior organization between language and social tasks found in our study replicates recent findings (Deen et al., 2015). The functional organization and specificity of the STS and TPJ has been a debated issue, due to the involvement of these regions in various cognitive domains (Carter and Huettel, 2013). Deen et al. suggested the existence of both task-selective regions and regions shared between several experimental conditions. Interestingly our conjunction analysis refines their report and draws a detailed antero-posterior functional atlas of the temporal lobe. While previous reviews evoked the possibility of a quite loose specialization of overlapping temporal areas (Carter and Huettel, 2013; Liebenthal et al., 2014), we found an organization based on specific and delineated contrast combinations reproducible at the individual level. Notably, we provided at the group level a picture of a fine functional multi-domains mosaic within the STS, with a series of nodes around which language and social contrasts are organized. Despite multiple contrasts activating the TPJ in our study, we still found with voxels that were not shared between contrasts neither at the group nor at the subject level, suggesting that nodes supporting common functions were surrounded by more specific clusters. Study of the corresponding local cortico-cortical connectivity will help to disentangle the existence of potential functional streams or converging pathways among the mechanisms of visuomotor, social/emotional and language domains. A side effect of our protocols dedicated to social cognition and visuomotor preparation was the activations covering the posterior part of the left middle occipitotemporal gyrus: notably the lateral occipital cortex, often reported as selective for object (Emberson et al., 2017), the EBA selective to body-related visual input but also in the comprehension of others' actions (Downing et al., 2001; Emberson et al., 2017), and the MT/V5 area important for the motion processing (Scheef et al., 2009). Indeed, together, the intentional triangles, the grasping and the saccades tasks involve various processes such as intention detection based on biological movement, motion detection, attentional shift, action preparation or perception, and object identification. A parcellation using functional data may help to the additional identification of all the associated areas (Thirion et al., 2014) beyond the tradition labels.

In the superior parietal cortex, we reported a functional organization similar to that previously described (Simon et al., 2002): the left AIP,

with anterior left-sided activation evoked by hand action and intentional triangles (Ramsey and Hamilton, 2010; Rozzi and Coudé, 2015) is followed by more posterior areas associated to grasping calculation and saccades tasks. Peaks of activity in this region revealed a complex organization of partially shared clusters between calculation and visuomotor tasks. Only the intentional triangles contrast did not show integration with any other contrasts. Considering the tight links between space, motor and number representations (Hubbard et al., 2005; Rossetti et al., 2004; Sawamura et al., 2002) the present database constitutes a significant advance for the comprehension of their cortical correlates.

Various parts of the frontal lobe were activated in the present study: specifically, the middle frontal gyrus was found to be organized in an anteroposterior succession of contrasts that were sensitive to social cues, emotional processing and action preparation. This extends the findings reported from a meta-analysis (Amodio and Frith, 2006; de la Vega et al., 2016; Paulesu et al., 1997). Organization of the inferior and dorsolateral frontal cortex could be described for the first time conjointly for visual, motor, social, emotional, language and computation tasks. Again, most of this region was covered in quite a complex pattern of task combinations and the ARCHI database provides a powerful tool to re-examine the specificity of frontal areas (Friederici, 2011). Finally, subcortical nuclei were evoked by various experimental situations, in particular the thalamus, the putamen, the caudate nuclei and the amygdala.

Another interesting marker for exploring the functional organization of the brain is the hemispheric lateralization. Here we observed some asymmetries typically reported in the literature: the left-lateralized ventral pathways for the VWFA and the left-sided perisylvian frontotemporal circuit for language processing (Broca and Wernicke areas) (Cai et al., 2008), the right-lateralized inferior temporal area for FFA (Kanwisher and Yovel, 2006) or a left anterior parietal area for motor task preparation (Tunik et al., 2005). This is an important prerequisite to explore the lateralization of human brain function. As an example, a previous analysis based on the present fMRI database used individual left activation for sentence reading as ROI jointly to the DTI data to show how the connectivity to language areas may constraint the hemispherical development of the VWFA (Bouhali et al., 2014).

Interestingly, we found voxels evoked by the false belief task independently from the modality in the posterior cingulate and the right TPJ specifically. It may be argued that the speed of the visual sentences makes the video task more difficult than its audio counterpart, thereby reducing the reliability of left TPJ activation (which was not present in 2/3 of subjects) and subsequent conjunction. However, involvement of the TPJ in the ToM representation has been more frequently reported in the right hemisphere than in the left (Lombardo et al., 2011; Mai et al., 2016; Saxe and Wexler, 2005). The use of a contrast conjunction probably helped to isolate the core support of the false belief processing. Our results raise the alternative possibility that the left-sided TPJ is modality-dependant, while the right one may be a correlate of an amodal ToM processing. Finally, our detailed multi-modal description of the temporal lobes revealed highly different organizations between left and right STS: the antero-posterior organization of the left side was not mirrored in the right one. The right STS seemed to present a lower degree of differentiated territories and we only reported one region of overlap, which never involved more than three contrasts. This is the first time that such a left/right difference of functional organization is presented all along the temporal sulci and jointly across a large number of cognitive fields. Whether it is caused by early anatomical differences of functional constraints during the development cannot be resolved here. However, accumulation of left/right differences in terms of Sylvian fissure length (Yeni-Komshian and Benson, 1976), cortical thickness (Plessen et al., 2014), sulcus depth (Leroy et al., 2015) and white matter tracts (Vernooij et al., 2007) in the temporal lobes suggests that differences in their functional organizations extend far beyond the well known language leftward lateralization. A next step is to study how such functional asymmetry reflects hemispheric structural differences.

A direct comparison of the functional mosaic presented here with the

literature was performed using the meta-analyses available on Neurosynth. It revealed that the cortical and subcortical regions evoked in our study are anatomically consistent with the literature. This is particularly clear in the temporal lobe and median regions. In both ARCHI and Neurosynth analysis, we found language-related activations (audio and video sentences) in the central part of the STS, surrounded posteriorly and anteriorly by activity related to social cognition (theory of mind, goal or intention attribution), while the very posterior part of the temporal gyrus hosted activity related to action, movement and saccade. In two anterior areas of the anterior prefrontal and orbitofrontal cortex, and one in the precuneus/pCC, results of the literature were replicated by the social cognition tasks of our localizer, whereas none of these areas were activated in any other condition. Similar observations could also be done along the iPS, with an anterior activation in relation to grasping and hand, and more posterior intermixed activations for visuospatial and calculation. Moreover, direct voxels correlations between ARCHI contrasts and Neurosynth images showed a high level of replication for a set of ARCHI tasks with the nearest corresponding terms in Neurosynth, such as the false belief, the video and audio sentences, calculation, saccade, rotation and the hand movement contrasts. For other tasks, we observed a clear tendency toward a domain-specific correlation, as the correlation matrix showed higher positive values along its diagonal while cross-domains mostly showed negative values (for instance social vs. visuo-motor related terms). Unsurprisingly, some of our tasks showed less specific patterns and correlated with various terms. For instance, the intention triangles contrast strongly correlated with meta-analyses calculated from 'face', 'reading', 'object' and 'motion'. This might reflect the large variety of cognitive processes elicited by the observation of animated objects when a social scene is detected (face-like processing, language based interpretation and so on). Likewise, the grasping contrast showed relevant correlation with, among others, 'object', 'hand' and 'action, which is a coherent decomposition onto the mechanisms required for such a task.

The specificity is of course lowered when neural circuits are highly intermixed, as in the case of frontoparietal functions such as calculation, saccade and mental rotation. This is also the limitation of comparing group analyses, especially when they are based on different experimental set-ups, protocols and sample sizes. A way to circumvent that is to infer the neural functions of these areas from the analysis of tasks similarities (conjunction) and differences (exclusion) at the individual level. For example, it could be argued that the partial similarity between cortical correlates of the eyes intention and the video sentences contrasts, supported by the ARCHI/Neurosynth matrix, may be explained by a more demanding lexical access in this social task than in the control gender task, and not by the gaze processing itself. However, we found a conjunction site between eyes intentions and intentional triangles contrasts (a passive observation which did not require any explicitly lexical decision) located posterior to the language correlates, These two tasks pointing to the concept (intentionality), we may hypothesize that this site was dedicated to the identification of intentions from distinct features (e.g. faces or movements).

Along the IPS, activations for grasping, calculation, rotation and saccade were largely overlapping, as was expected, considering that they may share partially common mechanisms and representations (Hubbard et al., 2005; McGuire and Sabes, 2011). Interestingly, while they overlap in a tiny cortical space, the number of conjunctions is limited and reproducible at the subject level. For instance, calculation shared voxels with the mental rotation, the saccades and the grasping contrasts. These zones of convergence may relate to common processes between quantity representation and spatial aptitude (Thompson et al., 2013), such as left/right shifts on the number line (Mathieu et al., 2016) and somatosensory roots of the numerical cognition (Krinzinger et al., 2011). In any case, they represent three distinct groups of voxels associated with different functional profiles and then may be segregated. As a third example, the left inferior frontal area is known to be particularly heterogeneous, and the Broca area was suspected to be essentially a collective term (Lindenberg et al., 2007). Indeed, it was recruited by at least one task from each of the three cognitive domains: audio and video sentences, grasping and two social tasks (trustworthiness and eyes intentions). Our database could enlighten the hypothesized developmental links between language and motor ability (Rizzolatti and Arbib, 1998), as well as between social communication skills and mirror neurons (Heiser et al., 2003; Iacoboni, 2009).

We should now consider a crucial issue for this type of multimodal database: are the isolated functional contrasts reliable at the single subject level? To benefit from the potential of the ARCHI database, we need to address new questions at the subject level to better understand how functional neural circuits are articulated, as we mentioned above concerning the use of conjunction, but also how they are organized in regard to the other available data: fiber tracks, myelin, cortical thickness, etc … Likewise, the short duration of our protocols make them a helpful tool for other studies, as long as they really capture an individual neural signature.

First, we found that in all experimental conditions, all of our 78 subjects' contrasts passed a minimal threshold of uncorrected $p < 0.01$ after task completion (8 or 10 trials). Considering the small number of trials, this liberal threshold could be accepted to isolate a relatively stable pattern. The evolution of the individual maps' significance revealed that all individual contrasts maps converged to a similar level of statistical strengths in a progressive way, ending with a small variance. This suggests that all subjects likely performed the experiments at similar levels of attention and performance, with no outlier or functional data loss. This point attests to the feasibility of the protocols as well as for the homogeneity of the obtained physiological data.

Second, in all the studied contrasts, within-subject inter-sessions' images correlations were about twice higher that inter-subjects' ones correlations. This demonstrates that functional patterns collected among different sessions for one subject performing a given task are more similar than those from different subjects, even if all of our tasks were likely to activate comparable neural networks in the population at the whole brain level as evidence by the ARCHI/Neurosynth comparison. When plotted in a reduced 3-D space, cluster of sessions belonging to the same subject could be easily visually identified, for instance in the eyes intention, the trustworthiness or the face gender contrast. Remarkably, the level of intra-subject similarity was quite stable across experimental conditions. Inter-subject differences increased with larger activation patterns, maybe involving more variable personal strategies. This also comforts that the quality of individual contrasts stay stable across tasks, and carry comparable individual neural signature. This consistency and homogeneity across fMRI data is a prerequisite if we want to study them in a fine grained way and tentatively explain local inter-subject variations.

The dense functional coverage of the cortex described above is also a promising situation to refine our comprehension of complex sulcus patterning, typically found in the left STS and TPJ region. Individual differences in the number of segments of the STS and morphological variability of its caudal branches (Segal and Petrides, 2012) make this region difficult to identify and to understand at the group level. Anatomical landmarks have been proposed to lower inter-subject differences (Fischl et al., 1999; Tucholka et al., 2012). In lateral occipital cortex and V5/MT area, it has also been proposed that sulci morphology may help for a reliable identification of functional areas (Dumoulin et al., 2000). Based on our findings, we could also consider the use of functional landmarks and nodes to characterize individual anatomical patterns and help improve anatomical labeling. The use of one of our localizers (Pinel et al., 2007) recently allowed to directly link morphological variability and functional activation related to hand action and sentence reading (Sun et al., 2016). This method could be directly applied on this new set of data in the posterior STS/TPJ region to understand how some functionally defined areas may be relevant to explain the underlying fiber distribution of shapes of sulci.

Describing the potential of our protocols and functional database, we

emphasized the presence of functional gradients, asymmetry, and overlaps. Indeed, describing the complex functional individual mosaic and extracting local organization requires the development of new tools to capture geometrical relations in a space-free system (Takerkart et al., 2014). Extracting spatial relationships between nearby activations may reveal particular individual designs such as antero-posterior organization functional gradients or mirror patterns, more relevant than space coordinates and potentially more robust across of subjects. This was recently stressed by the use of hyperalignment for between-subjects analysis, where individual brains were realigned using a large set of common response-tuning basis functions within a high-dimensional space (Guntupalli et al., 2016). Alignment based on resting state fMRI also allowed to identify common ROIs across subjects and improved statistical power for group analysis (Nenning et al., 2017). All these approaches point out the necessity to overcome the limitation of comparisons based on macro-anatomy only. On the contrary, these topological functional mappings should be fed by the microstructure maps of local connections provided by the ARCHI database.

The functional localizers developed for this project (available at https://philippepinel.wixsite.com/localizers) provided an efficient mapping of various and important cerebral circuits in adults from the general population. These short protocols successfully performed by 100% of our subjects. The modular design may allow expanding such a functional database easily and at a low cost. We have benefited from the experience developed with the Pinel et al. (2007) localizer, which was shared among various laboratories in the last decade and translated into 7 languages (http://www.neurospin-wiki.org/pmwiki/Main/StandardLocalizers). Considering the range of tasks addressed in this database, our localizers could also be relevant and applied (or slightly adapted) to clinical populations to test for any differences in one of the explored cognitive domains, or to identify specific cerebral regions. In particular, atypical neural circuits of patients suffering from dyslexia, dyscalculia, various forms of autism or neurodevelopmental disorders could be easily investigated and compared to our control cohort. Group analyses reported in the present article are available on our website and may already serve as independent ROI for finer explorations (Poldrack, 2007). New material, publications and links will also be added to the website as part of an ongoing process (new analyses, updated preprocessing, new data collected from other centers). Similarly, pre-scan training and post-scan debriefing could also be downloaded from our website to ensure the quality of fMRI data.

For each subject, genetic data was collected but not analyzed in this introducing article. We previously demonstrated that the effect of candidate genes onto fMRI endophenotype could be successfully identified on a relatively small population (based 96 subjects from the Pinel et al., 2007 localizer only). While such sample sizes could not compete with genome-wide association studies, this example advocates for more focused fMRI/genetic association to address a specific issue. We hope to extend the ARCHI functional database in the future to accumulate more functional and genetic data, thus increasing the power of association analyses. Aggregating samples from various centers could be expected to increase the fRMI/genetic collection as a continuation of the project. Several genes involved in developmental disorders, abilities, or affecting behavioral scores of language, calculation, visuomotor and social skills have been reported (Baron-Cohen et al., 2014; Docherty et al., 2010; Taschereau-Dumouchel et al., 2016). By targeting these candidate genes, we hope to explore how and where they may alter the development of healthy brains, notably for social tasks (false belief, intentional triangles and eyes intention contrasts) which have been previously reported affected in patient population (Autism and Asperger syndrome) (Baron-Cohen et al., 1999; Castelli et al., 2002; Leekam and Perner, 1991).

The ARCHI project is an additional contribution to the restricted set of large functional databases available to the community, such as the Human Connectome Project (http://www.humanconnectomeproject.org) (Barch et al., 2013) for adults and IMAGEN project (http://www.imagen-europe.com) (Schumann et al., 2010) for adolescents. Even

though merging these collections is still challenging (Amunts et al., 2014), the complementarity or similarity of these projects' tasks with ours will be important in the future to be able to generalize results or making inferences/predictions derived from one experimental context onto another one (functional nodes, parcellation, geometry of functional organization, etc.). A first important step to diffuse the database and local tools to the neuroscience community has been done in sharing data within the Human Brain Project (HBP) network (https://www.humanbrainproject.eu). This ten-year international scientific project aims to develop a realistic simulation of the human brain, based on empirical data and detailed models. In this context, the present fMRI database was delivered as material to feed the project and develop new methodologies. One recent extension of this localizer/databasing work is the IBC dataset (Pinho et al., 2018). The IBC project is a longitudinal study that aims to scan extensively and at high-resolution an individual performing a large range of tasks. Considering the efficiency and reliability of our ARCHI protocols, they served as a foundation to initiate this new fMRI collection. IBC data will be soon available on the HBP servers and collaboration could also be stimulated on this base.

In conclusion, we summarized the methods and potential of the functional part of the ARCHI database. We introduced the four fMRI localizers designed for a fast and efficient subject level exploration within the field of language, social cognition, visuomotor skills and mathematics. For anatomical-based studies, some of them can be used independently to map almost entirely the frontal lobe, the superior parietal cortex, the temporal gyrus or the medial surface of cerebral hemispheres. As these protocols have already been shared and their use begins to grow in the scientific community, we hope that their diffusion will encourage collaboration to extend such a homogenous collection. The present fMRI database, in relation to the individual structural measurements, should already stimulate new methodical approaches to address the richness of the brain phenotypes and to extend the collection thanks to the diffusion of tools.

Acknowledgements

Appendix A. Supplementary data

Supplementary data to this article can be found online at https://doi.org/10.1016/j.neuroimage.2019.04.056.

References

Amodio, D.M., Frith, C.D., 2006. Meeting of minds: the medial frontal cortex and social cognition. Nat. Rev. Neurosci. 7, 268.

Amunts, K., Hawrylycz, M.J., Van Essen, D.C., Van Horn, J.D., Harel, N., Poline, J.-B., De Martino, F., Bjaalie, J.G., Dehaene-Lambertz, G., Dehaene, S., 2014. Interoperable atlases of the human brain. Neuroimage 99, 525–532.

Assaf, Y., Alexander, D.C., Jones, D.K., Bizzi, A., Behrens, T.E., Clark, C.A., Cohen, Y., Dyrby, T.B., Huppi, P.S., Knoesche, T.R., 2013. The CONNECT project: combining macro-and micro-structure. Neuroimage 80, 273–282.

Barch, D.M., Burgess, G.C., Harms, M.P., Petersen, S.E., Schlaggar, B.L., Corbetta, M., Glasser, M.F., Curtiss, S., Dixit, S., Feldt, C., 2013. Function in the human connectome: task-fMRI and individual differences in behavior. Neuroimage 80, 169–189.

Baron-Cohen, S., Jolliffe, T., Mortimore, C., Robertson, M., 1997. Another advanced test of theory of mind: evidence from very high functioning adults with autism or Asperger syndrome. JCPP (J. Child Psychol. Psychiatry) 38, 813–822.

Baron-Cohen, S., Leslie, A.M., Frith, U., 1985. Does the autistic child have a "theory of mind"? Cognition 21, 37–46.

Baron-Cohen, S., Murphy, L., Chakrabarti, B., Craig, I., Mallya, U., Lakatošová, S., Rehnstrom, K., Peltonen, L., Wheelwright, S., Allison, C., 2014. A genome wide association study of mathematical ability reveals an association at chromosome 3q29, a locus associated with autism and learning difficulties: a preliminary study. PLoS One 9, e96374.

Baron-Cohen, S., Ring, H., Wheelwright, S., Bullmore, E., Brammer, M., Simmons, A., Williams, S., 1999. Social intelligence in the normal and autistic brain: an fMRI study. Eur. J. Neurosci. 11, 1891.

Behrens, T., Jenkinson, M., Robson, M., Smith, S., Johansen-Berg, H., 2006. A consistent relationship between local white matter architecture and functional specialisation in medial frontal cortex. Neuroimage 30, 220–227.

Belin, P., Zatorre, R.J., Lafaille, P., Ahad, P., Pike, B., 2000. Voice-selective areas in human auditory cortex. Nature 403, 309–312.

Bouhali, F., de Schotten, M.T., Pinel, P., Poupon, C., Mangin, J.-F.o., Dehaene, S., Cohen, L., 2014. Anatomical connections of the visual word form area. J. Neurosci. 34, 15402–15414.

Cai, Q., Lavidor, M., Brysbaert, M., Paulignan, Y., Nazir, T.A., 2008. Cerebral lateralization of frontal lobe language processes and lateralization of the posterior visual word processing system. J. Cogn. Neurosci. 20, 672–681.

Carter, R.M., Huettel, S.A., 2013. A nexus model of the temporal-parietal junction. Trends Cognit. Sci. 17, 328–336.

Castelli, F., Frith, C., Happé, F., Frith, U., 2002. Autism, Asperger syndrome and brain mechanisms for the attribution of mental states to animated shapes. Brain 125, 1839–1849.

Castelli, F., Happé, F., Frith, U., Frith, C., 2000. Movement and mind: a functional imaging study of perception and interpretation of complex intentional movement patterns. Neuroimage 12, 314–325.

Cohen, L., Dehaene, S., 2004. Specialization within the ventral stream: the case for the visual word form area. Neuroimage 22, 466–476.

Cohen, M.S., Kosslyn, S.M., Breiter, H.C., DiGirolamo, G.J., Thompson, W.L., Anderson, A., Bookheimer, S., Rosen, B.R., Belliveau, J., 1996. Changes in cortical activity during mental rotation A mapping study using functional MRI. Brain 119, 89–100.

Culham, J.C., Kanwisher, N.G., 2001. Neuroimaging of cognitive functions in human parietal cortex. Curr. Opin. Neurobiol. 11, 157–163.

de la Vega, A., Chang, L.J., Banich, M.T., Wager, T.D., Yarkoni, T., 2016. Large-scale meta-analysis of human medial frontal cortex reveals tripartite functional organization. J. Neurosci. 36, 6553–6562.

Decety, J., Lamm, C., 2007. The role of the right temporoparietal junction in social interaction: how low-level computational processes contribute to meta-cognition. Neuroscientist 13, 580–593.

Deen, B., Koldewyn, K., Kanwisher, N., Saxe, R., 2015. Functional organization of social perception and cognition in the superior temporal sulcus. Cerebr. Cortex 25, 4596–4609.

Docherty, S.J., Davis, O., Kovas, Y., Meaburn, E., Dale, P.S., Petrill, S.A., Schalkwyk, L., Plomin, R., 2010. A genome-wide association study identifies multiple loci associated with mathematics ability and disability. Genes Brain Behav. 9, 234–247.

Downing, P.E., Jiang, Y., Shuman, M., Kanwisher, N., 2001. A cortical area selective for visual processing of the human body. Science 293, 2470–2473.

Dumoulin, S.O., Bittar, R.G., Kabani, N.J., Baker Jr., C.L., Le Goualher, G., Pike, G.B., Evans, A.C., 2000. A new anatomical landmark for reliable identification of human area V5/MT: a quantitative analysis of sulcal patterning. Cerebr. Cortex 10, 454–463.

Emberson, L.L., Crosswhite, S.L., Richards, J.E., Aslin, R.N., 2017. The lateral occipital cortex (LOC) is selective for object shape, not texture/color, at 6 months. J. Neurosci. 3300–3316.

Fischl, B., Sereno, M.I., Tootell, R.B., Dale, A.M., 1999. High-resolution intersubject averaging and a coordinate system for the cortical surface. Hum. Brain Mapp. 8, 272–284.

Fletcher, P.C., Happé, F., Frith, U., Baker, S.C., Dolan, R.J., Frackowiak, R.S.J., Frith, C.D., 1995. Other minds in the brain: a functional imaging study of "theory of mind" in story comprehension. Cognition 57, 109–128.

Friederici, A.D., 2011. The brain basis of language processing: from structure to function. Physiol. Rev. 91, 1357–1392.

Friston, K.J., Holmes, A.P., Price, C., Büchel, C., Worsley, K., 1999. Multisubject fMRI studies and conjunction analyses. Neuroimage 10, 385–396.

Guntupalli, J.S., Hanke, M., Halchenko, Y.O., Connolly, A.C., Ramadge, P.J., Haxby, J.V., 2016. A model of representational spaces in human cortex. Cerebr. Cortex 26, 2919–2934.

Heider, F., Simmel, M., 1944. An experimental study of apparent behavior. Am. J. Psychol. 57, 243–259.

Hein, G., Knight, R.T., 2008. Superior temporal sulcus - it's my area: or is it? J. Cogn. Neurosci. 20, 2125–2136.

Heiser, M., Iacoboni, M., Maeda, F., Marcus, J., Mazziotta, J.C., 2003. The essential role of Broca's area in imitation. Eur. J. Neurosci. 17, 1123–1128.

Hill, J., Dierker, D., Neil, J., Inder, T., Knutsen, A., Harwell, J., Coalson, T., Van Essen, D., 2010. A surface-based analysis of hemispheric asymmetries and folding of cerebral cortex in term-born human infants. J. Neurosci. 30, 2268–2276.

Hubbard, E.M., Piazza, M., Pinel, P., Dehaene, S., 2005. Interactions between number and space in parietal cortex. Nat. Rev. Neurosci. 6, 435–448.

Iacoboni, M., 2009. Imitation, empathy, and mirror neurons. Annu. Rev. Psychol. 60, 653–670.

Jordan, K., Heinze, H.-J., Lutz, K., Kanowski, M., Jäncke, L., 2001. Cortical activations during the mental rotation of different visual objects. Neuroimage 13, 143–152.

Kanwisher, N., Yovel, G., 2006. The fusiform face area: a cortical region specialized for the perception of faces. Phil. Trans. Biol. Sci. 361, 2109.

Kosslyn, S.M., Digirolamo, G.J., Thompson, W.L., Alpert, N.M., 1998. Mental rotation of objects versus hands: neural mechanisms revealed by positron emission tomography. Psychophysiology 35, 151–161.

Krinzinger, H., Koten, J.W., Horoufchin, H., Kohn, N., Arndt, D., Sahr, K., Konrad, K., Willmes, K., 2011. The role of finger representations and saccades for number processing: an fMRI study in children. Front. Psychol. 2, 373.

Laumann, T.O., Gordon, E.M., Adeyemo, B., Snyder, A.Z., Joo, S.J., Chen, M.-Y., Gilmore, A.W., McDermott, K.B., Nelson, S.M., Dosenbach, N.U., 2015. Functional system and areal organization of a highly sampled individual human brain. Neuron 87, 657–670.

Leekam, S.R., Perner, J., 1991. Does the autistic child have a metarepresentational deficit? Cognition 40, 203–218.

Leroy, F., Cai, Q., Bogart, S.L., Dubois, J., Coulon, O., Monzalvo, K., Fischer, C., Glasel, H., Van der Haegen, L., Bénézit, A., Ching-Po, L., David, N.,K., Aya, S.,I., Lucie, H.-P., Marie-Laure, M., Cyril, P., Marc, B., Neil, R., William, D.,H., Jean-François, M., Ghislaine, D.-L., 2015. New human-specific brain landmark: the depth asymmetry of superior temporal sulcus. Proc. Natl. Acad. Sci. Unit. States Am. 112, 1208–1213.

Liebenthal, E., Desai, R.H., Humphries, C., Sabri, M., Desai, A., 2014. The functional organization of the left STS: a large scale meta-analysis of PET and fMRI studies of healthy adults. Front. Neurosci. 8.

Lindenberg, R., Fangerau, H., Seitz, R.J., 2007. "Broca's area" as a collective term? Brain Lang. 102, 22–29.

Lombardo, M.V., Chakrabarti, B., Bullmore, E.T., Baron-Cohen, S., Consortium, M.A., 2011. Specialization of right temporo-parietal junction for mentalizing and its relation to social impairments in autism. Neuroimage 56, 1832–1838.

Lundqvist, D., Flykt, A., Öhman, A., 1998. The Karolinska Directed Emotional Faces (KDEF). CD ROM from Department of Clinical Neuroscience. Psychology Section. Karolinska Institutet, 1998. ISBN 91-630-7164-9.

Mai, X., Zhang, W., Hu, X., Zhen, Z., Xu, Z., Zhang, J., Liu, C., 2016. Using tDCS to explore the role of the right temporo-parietal junction in theory of mind and cognitive empathy. Front. Psychol. 7, 380.

Mathieu, R., Gourjon, A., Couderc, A., Thevenot, C., Prado, J.r.m., 2016. Running the number line: rapid shifts of attention in single-digit arithmetic. Cognition 146, 229–239.

McGuire, L.M., Sabes, P.N., 2011. Heterogeneous representations in the superior parietal lobule are common across reaches to visual and proprioceptive targets. J. Neurosci. 31, 6661–6673.

Miller, M.B., Donovan, C.-L., Van Horn, J.D., German, E., Sokol-Hessner, P., Wolford, G.L., 2009. Unique and persistent individual patterns of brain activity across different memory retrieval tasks. Neuroimage 48, 625–635.

Nadeau, S.E., Williamson, D., Crosson, B., Rothi, L.J.G., Heilman, K.M., 1998. Functional imaging: heterogeneity in task strategy and functional anatomy and the case for individual analysis. Cogn. Behav. Neurol. 11, 83–96.

Nenning, K.-H., Liu, H., Ghosh, S.S., Sabuncu, M.R., Schwartz, E., Langs, G., 2017. Diffeomorphic functional brain surface alignment: functional demons. Neuroimage 156, 456–465.

Ochiai, T., Grimault, S., Scavarda, D., Roch, G., Hori, T., Riviere, D., Mangin, J.F.o., RÃ©gis, J., 2004. Sulcal pattern and morphology of the superior temporal sulcus. Neuroimage 22, 706–719.

Oosterhof, N.N., Todorov, A., 2008. The functional basis of face evaluation. Proc. Natl. Acad. Sci. Unit. States Am. 105, 11087–11092.

Paulesu, E., Goldacre, B., Scifo, P., Cappa, S.F., Gilardi, M.C., Castiglioni, I., Perani, D., Fazio, G., 1997. Functional heterogeneity of left inferior frontal cortex as revealed by fMRI. Neuroreport 8, 2011–2016.

Perner, J., Aichhorn, M., 2008. Theory of mind, language and the temporoparietal junction mystery. Trends Cognit. Sci. 12, 123–126.

Pinel, P., Fauchereau, F., Moreno, A., Barbot, A., Lathrop, M., Zelenika, D., Le Bihan, D., Poline, J.B., Bourgeron, T., Dehaene, S., 2012. Genetic variants of FOXP2 and KIAA0319/TTRAP/THEM2 locus are associated with altered brain activation in distinct language-related regions. J. Neurosci. 32, 817–825.

Pinel, P., Thirion, B., Meriaux, S., Jobert, A., Serres, J., Le Bihan, D., Poline, J.B., Dehaene, S., 2007. Fast reproducible identification and large-scale databasing of individual functional cognitive networks. BMC Neurosci. 8, 91.

Pinho, A.L., Amadon, A., Ruest, T., Fabre, M., Dohmatob, E., Denghien, I., Ginisty, C., Becuwe-Desmidt, S., Roger, S., Laurier, L., Doublé, C., Martins, B., Pinel, P., Eger, E., Varoquaux, G., Pallier, C., Dehaene, S., Hertz-Pannier, L., Thirion, B., 2018. Individual Brain Charting, a high-resolution fMRI dataset for cognitive mapping. Sci. Data 5.

Plessen, K.J., Hugdahl, K., Bansal, R., Hao, X., Peterson, B.S., 2014. Sex, age, and cognitive correlates of asymmetries in thickness of the cortical mantle across the life span. J. Neurosci. 34, 6294–6302.

Poldrack, R.A., 2007. Region of interest analysis for fMRI. Soc. Cognit. Affect Neurosci. 2, 67–70.

Power, J.D., Barnes, K.A., Snyder, A.Z., Schlaggar, B.L., Petersen, S.E., 2012. Spurious but systematic correlations in functional connectivity MRI networks arise from subject motion. Neuroimage 59, 2142–2154.

Putnam, M.C., Steven, M.S., Doron, K.W., Riggall, A.C., Gazzaniga, M.S., 2010. Cortical projection topography of the human splenium: hemispheric asymmetry and individual differences. J. Cogn. Neurosci. 22, 1662–1669.

Raichle, M.E., MacLeod, A.M., Snyder, A.Z., Powers, W.J., Gusnard, D.A., Shulman, G.L., 2001. A default mode of brain function. Proc. Natl. Acad. Sci. Unit. States Am. 98, 676–682.

Ramsey, R., Hamilton, A.F.de C., 2010. Understanding actors and object-goals in the human brain. Neuroimage 50, 1142–1147.

Rizzolatti, G., Arbib, M.A., 1998. Language within our grasp. Trends Neurosci. 21, 188–194.

Rossetti, Y., Jacquin-Courtois, S., Rode, G., Ota, H., Michel, C., Boisson, D., 2004. Does action make the link between number and space representation? Visuo-manual adaptation improves number bisection in unilateral neglect. Psychol. Sci. 15, 426–430.

Rozzi, S., Coudé, G., 2015. Grasping actions and social interaction: neural bases and anatomical circuitry in the monkey. Front. Psychol. 6, 973.

Rusconi, E., Pinel, P., Eger, E., LeBihan, D., Thirion, B., Dehaene, S., Kleinschmidt, A., 2009. A disconnection account of Gerstmann syndrome: functional neuroanatomy evidence. Ann. Neurol. 66, 654–662.

Sawamura, H., Shima, K., Tanji, J., 2002. Numerical representation for action in the parietal cortex of the monkey. Nature 415, 918.

Saxe, R., 2006. Uniquely human social cognition. Curr. Opin. Neurobiol. 16, 235–239.

Saxe, R., Kanwisher, N., 2003. People thinking about thinking people: the role of the temporo-parietal junction in "theory of mind". Neuroimage 19, 1835–1842.

Saxe, R., Wexler, A., 2005. Making sense of another mind: the role of the right temporo-parietal junction. Neuropsychologia 43, 1391–1399.

Saygin, Z.M., Osher, D.E., Koldewyn, K., Reynolds, G., Gabrieli, J.D., Saxe, R.R., 2012. Anatomical connectivity patterns predict face selectivity in the fusiform gyrus. Nat. Neurosci. 15, 321–327.

Scheef, L., Boecker, H., Daamen, M., Fehse, U., Landsberg, M.W., Granath, D.-O., Mechling, H., Effenberg, A.O., 2009. Multimodal motion processing in area V5/MT: evidence from an artificial class of audio-visual events. Brain Res. 1252, 94–104.

Schumann, G., Loth, E., Banaschewski, T., Barbot, A., Barker, G., Büchel, C., Conrod, P., Dalley, J., Flor, H., Gallinat, J., Garavan, H., Heinz, A., Itterman, B., Lathrop, M., Mallik, C., Mann, K., Martinot, J.L., Paus, T., Poline, J.B., Robbins, T.W., Rietschel, M., Reed, L., Smolka, M., Spanagel, R., Claudia, S., Stephens, D.N., Ströhle, A., Struve, M., consortium, t.I., 2010. The IMAGEN study: reinforcement-related behaviour in normal brain function and psychopathology. Mol. Psychiatr. 15, 1128.

Segal, E., Petrides, M., 2012. The morphology and variability of the caudal rami of the superior temporal sulcus. Eur. J. Neurosci. 36, 2035–2053.

Simon, O., Kherif, F., Flandin, G., Poline, J.B., Riviere, D., Mangin, J.F., Le Bihan, D., Dehaene, S., 2004. Automated clustering and functional geometry of human parietofrontal networks for language, space, and number. Neuroimage 23, 1192–1202.

Simon, O., Mangin, J.F., Cohen, L., Le Bihan, D., Dehaene, S., 2002. Topographical layout of hand, eye, calculation, and language-related areas in the human parietal lobe. Neuron 33, 475–487.

Sun, Z., Pinel, P., Rivière, D., Moreno, A., Dehaene, S., Mangin, J.-F., 2016. Linking morphological and functional variability in hand movement and silent reading. Brain Struct. Funct. 221, 3361–3371.

Takerkart, S., Auzias, G., Thirion, B., Ralaivola, L., 2014. Graph-based inter-subject pattern analysis of fMRI data. PLoS One 9, e104586.

Taschereau-Dumouchel, V., Hétu, S., Michon, P.-E., Vachon-Presseau, E., Massicotte, E., De Beaumont, L., Fecteau, S., Poirier, J., Mercier, C., Chagnon, Y.C., 2016. BDNF val 66 met polymorphism influences visuomotor associative learning and the sensitivity to action observation. Sci. Rep. 6, 34907.

Thirion, B., Pinel, P., Mériaux, S., Roche, A., Dehaene, S., Poline, J.-B., 2007. Analysis of a large fMRI cohort: statistical and methodological issues for group analyses. Neuroimage 35, 105–120.

Thirion, B., Varoquaux, G.l., Dohmatob, E., Poline, J.-B., 2014. Which fMRI clustering gives good brain parcellations? Front. Neurosci. 8, 167.

Thompson, J.M., Nuerk, H.-C., Moeller, K., Kadosh, R.C., 2013. The link between mental rotation ability and basic numerical representations. Acta Psychol. 144, 324–331.

Tucholka, A., Fritsch, V., Poline, J.-B., Thirion, B., 2012. An empirical comparison of surface-based and volume-based group studies in neuroimaging. Neuroimage 63, 1443–1453.

Tunik, E., Frey, S.H., Grafton, S.T., 2005. Virtual lesions of the anterior intraparietal area disrupt goal-dependent on-line adjustments of grasp. Nat. Neurosci. 8, 505.

van den Heuvel, M.P., Sporns, O., 2013. Network hubs in the human brain. Trends Cognit. Sci. 17, 683–696.

Van Essen, D.C., Ugurbil, K., Auerbach, E., Barch, D., Behrens, T., Bucholz, R., Chang, A., Chen, L., Corbetta, M., Curtiss, S.W., 2012. The Human Connectome Project: a data acquisition perspective. Neuroimage 62, 2222–2231.

Vernooij, M., Smits, M., Wielopolski, P., Houston, G., Krestin, G., van der Lugt, A., 2007. Fiber density asymmetry of the arcuate fasciculus in relation to functional hemispheric language lateralization in both right-and left-handed healthy subjects: a combined fMRI and DTI study. Neuroimage 35, 1064–1076.

Wager, T.D., Nichols, T.E., 2003. Optimization of experimental design in fMRI: a general framework using a genetic algorithm. Neuroimage 18, 293–309.

Wimmer, H., Perner, J., 1983. Beliefs about beliefs: representation and constraining function of wrong beliefs in young children's understanding of deception. Cognition 13, 103–128.

Winston, J., Strange, B., O'Doherty, J., Dolan, R., 2002. Automatic and intentional brain responses during evaluation of trustworthiness of faces. Nat. Neurosci. 277–283.

Yarkoni, T., Poldrack, R.A., Nichols, T.E., Van Essen, D.C., Wager, T.D., 2011. Large-scale automated synthesis of human functional neuroimaging data. Nat. Methods 8, 665.

Yeni-Komshian, G.H., Benson, D.A., 1976. Anatomical study of cerebral asymmetry in the temporal lobe of humans, chimpanzees, and rhesus monkeys. Science 192, 387–389.

Zlatkina, V., Petrides, M., 2014. Morphological patterns of the intraparietal sulcus and the anterior intermediate parietal sulcus of Jensen in the human brain. Proc. Biol. Sci. 281.